Modelling of Stiffness and Hygroexpansion of Wood Fibre Composites

Stålne, Kristian

2001

Document Version:
Förlagets slutgiltiga version

LUND UNIVERSITY

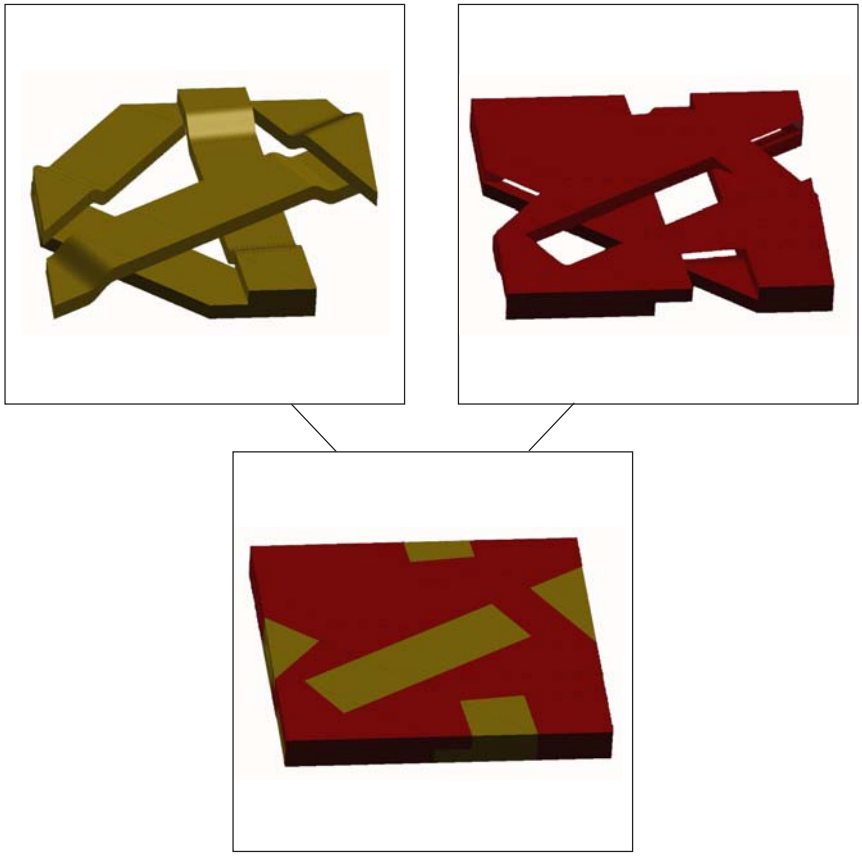

MODELLING OF STIFFNESS AND HYGROEXPANSION OF WOOD FIBRE COMPOSITES

KRISTIAN STÅLNE

Structural Mechanics

Licentiate Dissertation

Structural Mechanics

ISRN LUTVDG/TVSM--01/3061--SE (1-92)
ISSN 0281-6679

MODELLING OF STIFFNESS AND HYGROEXPANSION OF WOOD FIBRE COMPOSITES

KRISTIAN STÅLNE

Printed by KFS I Lund AB, Lund, Sweden, November 2001.

For information, address:
Division of Structural Mechanics, LTH, Lund University, Box 118, SE-221 00 Lund, Sweden.
Homepage: http://www.byggmek.lth.se

Preface

The work presented in this dissertation was carried out during the period 1998-2001 at the Division of Structural Mechanics, Department of Building and Environmental Technology, Lund University, Sweden. The financial support by the Swedish Foundation for Strategical Research (SSF) programme "Wood Technology" is gratefully acknowledged.

I would like to thank my supervisor, Prof. Per Johan Gustafsson, for his patience, encouragement, for always having time for discussions and for being a very skilful supervisor. I also would like to thank Kent, Erik, Peter, Jonas, Per-Anders and the rest of the staff at the structural mechanics division for always helping me when I am in conflict with my computer and for making this working environment very pleasant.

Special thanks go to Dr. Dennis Rasmusson and Dr. Bijan Adl Zarrabi for good collaboration and for the practical training period I spent at Perstorp AB and to Dr. Håkan Wernersson at Pergo AB for valuble discussions.

I finally would like to thank my family and friends and the rest of my "pack" consisting of Jenny and Ruben for all support and encouragement.

Lund, November 2001

Kristian Stålne

Contents

Summary of papers 1-4

Paper 1 The field of research involving the analytical modelling of the stiffness and hygroexpansion of composite material is reviewed. This paper can be regarded as an introduction to the area of the mechanics of composite materials in general and to wood fibre composites in particular. The most important models, such as the Reuss and Voigt bounds and the Halpin-Tsai, are described, along with their advantages and limitations. The report also contains examples of calculations made for various models, allowing them to be compared.

Paper 2 In this paper, coordinate transformations of the stresses, strains and stiffness of composite materials are described. A new method for interpolating between the extremes of homogeneous strain and homogeneous stress for calculating the stiffness matrix of composites is introduced. This new interpolation method is shown by use of advanced matrix theory, to be coordinate independent.

Paper 3 A 3D analytical model for stiffness and hygroexpansion is presented. The model involves two steps. The first step is the homogenisation of a structure composed of a single wood fibre coated by a layer of matrix material. The second step is the integration of the various fibre orientations involving a linear and an exponential interpolation between an extreme case of homogenous strain and an extreme case of homogenous stress. A comparison is made between the prediction as modelled and measurement data for stiffness, Poisson's ratio and hygroexpansion. The matrix material is assumed to have isotropic properties, whereas the fibres and the particle material can have arbitrary orthotropic properties. The model can be used for all volume fractions and is also valid for particle composites.

Paper 4 This paper presents a 3D numerical model for the stiffness and hygroexpansion properties of wood fibre composite materials. The microstructure of a composite composed of a number of fibres is modelled by use of a fibre geometry preprocessor. The model is employed for analysing the mechanical behaviour of wood fibre composites that have fibre network geometries. Results obtained by use of the model are compared with results based on the analytical model presented in paper 3 and with various test results.

Introduction

1 Background

Wood composite materials are gaining in popularity, both for environmental reasons and because of their high performance-to-cost ratio. A matter that is often a drawback, however, when wood products are employed is their shape instability when subjected to a change or a gradient in moisture content. This is of considerable importance for both solid timber and wood-based composite materials. At the same time, there are important differences between composites and solid timber. One of these is the greater variability found in a timber structural member due to knots, grain deviations, etc, making predictions of shape instability and other properties uncertain. Another difference is in the possibility of designing a composite for uses of specific types. Wood composite materials can be designed to be of very differing properties in terms of strength and stiffness, product dimensions, heat insulation properties, sound muffling, durability, shape stability etc.

The design or improvement of a composite material, whether it already exists or is only being considered for possible manufacture, is very much facilitated by access to some form of calculation model that enables analysis and predictions of the performance of the material to be made. Access to a general and accurate tool for analysing and predicting the load and the moisture induced deformations of a composite material would certainly be of great value and would promote the use of wood composites.

The orthotropic and moisture-sensitive nature of wood materials has led to difficulties in modelling their mechanical behaviour. Even in the case of linear elasticity there are nine independent stiffness constants and three independent hygroexpansion parameters that need to be taken account of. In modelling wood composites, one has to also take the structure of the material, including the shape of the wood fibres or of the wood particle, the matrix properties and the fibre-matrix interaction, into consideration. Studying the literature on composite material modelling, it is evident that the more complicated a composite is, the less interest there is in modelling it.

The possibilities of finite element analysis have been increased very much by developments in computer performance. It is possible now to analyse complex structures by use of fairly detailed models. Finite element analysis is used today for the continuum modelling of moisture-induced deformations of solid wood members [3]. The detailed FE-modelling of wood fibres and of the heterogeneous

structure of small pieces of wood has been used to analyse the influence of the microstructure of wood on its global homogenised properties [2]. However, even if the performance of today's computers is impressive, in the foreseeable future it would still appear possible to model only very small volumes of a heterogeneous composite material structure. Analytical composite material modelling is generally, more convenient to apply, but in some cases the results are more of an approximate character.

2 Scope of the Present Work

The work presented in this licentiate dissertation is the first part of a PhD project aiming at developing a computational tool allowing the global deformation properties of wood fibres or of particle composite materials and products to in theory be predicted from the known properties of their constituents, as well as the structure of the composite material. Achieving this overall goal involves two basic steps. The first step is to create a model of the microstructure of wood fibre composite materials, making it possible to analyse the global deformations of small pieces of the composite material when exposed to homogeneous states of climate and to mechanical load. This concerns the rate- and time-independent performance of the materials, as presented in this report. Numerical examples and experimental verifications of high pressure laminates, HPL, used in such applications as flooring [1], are presented in Figure 1.

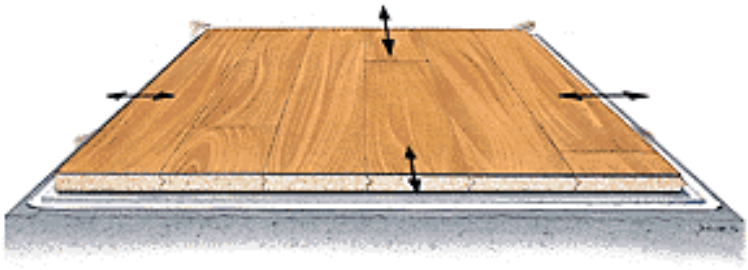

Figure 1: *HPL floor under hygroexpansion.*

The present licentiate dissertation is composed of four papers. In paper 1 the research area of composite material stiffness and of hygroexpansion modelling is reviewed. Paper 2 deals with coordinate transformations, an analytical interpolation method being introduced and investigated thoroughly. The method described is used in paper 3 in connection with the presentation of a complete analytical homogenisation model. Finally, in paper 4, a finite element model of an HPL is described and is compared with results obtained by use of this

analytical model and with various test results.

3 Future Work

The major part of the second step in the PhD project will be to create a continuum mechanics model of the deformation properties of a composite material. The parameter values for use in this model are to be obtained by use of a numerical microstructure model or of an analytical composite material model. Time-dependent properties such as creep and mechanosorption will also be implemented first in a micromechanics model and then in a continuum mechanics model. By means of this material model and of the finite element method it will be possible to calculate the moisture-induced deformations of products made of wood composites when exposed to various loading conditions and climatic conditions.

References

[1] Adl Zarrabi, B. (1998). *Hygro-Elastic Deformation of High Pressure Laminates.* Doctoral thesis, Division of Building Material, Chalmers University of Technology, Sweden

[2] Persson, K. (2001). *Micromechanical modelling of wood and fibre properties.* Doctoral thesis, Division of Structural Mechanics, Lund University, Sweden.

[3] Ormarsson, S. (1999). *Numerical Analysis of Moisture-Related Distortions in Sawn Timber.* Doctoral Thesis, Division of Structural Mechanics, Chalmers University of Technology, Sweden.

I

Review of Analytical Models for Stiffness and Hygroexpansion of Composite Materials

Kristian Stålne
Division of Structural Mechanics
Lund University, Sweden

1 Introduction

1.1 Contents of the report

This report is an overview of analytical models for stiffness and hygroexpansion analysis of composite materials. The most important linear elastic models are presented and discussed. In the first section different composite materials are defined and described, with emphasis being placed on wood fibre composites. The concept of homogenisation, the reason for homogenising a composite material and ways of doing so are then discussed. Important advances recently in the field of composite homogenisation are described briefly. The models most frequently used for the homogenisation of the stiffnesses are then examined, the important issue of calculating hygroexpansion properties being taken up. Finally examples are provided of stiffness and hygroexpansion calculations for a high pressure laminate. References is also made in this report to various other useful and comprehensive reviews of research in the area of the composite material mechanics.

1.2 Definition of a composite material

A composite material is created when two or more materials are mixed in order to achieve different properties than those of its constituents. The regions occupied by the seperate constituents are considered as being homogeneous continua and are commonly assumed to be bonded together firmly at the respective interfaces. The main advantage of using a composite material is that it can be tailor-made for a particular application. By adding fibres aligned in one preferred direction, the material can be made stiffer and stronger in that direction. This makes it possible to achieve light but stiff materials. Different types of composite materials can be distinguished on the basis of their function and of the structural geometry of the material: particle composites, fibre composites, laminate composites and composites with irregular geometry, according to Figure 1 which is taken from [30]. The particle composite most frequently employed is concrete. There, cement is mixed with sand and small stones to produce a material that is cheaper and has improved properties, such as having lesser moisture-induced strains. Reinforcing concrete with steel rods provides it a high degree of strength, also when under tension. Concrete can also be reinforced with steel or glass fibres, making it a fibre composite as well [25]. Laminate composites are created by placing thin isotropic or anisotropic plates or laminas, on top each other, making it easier to control the stiffness.

Fibre composites are often classified by the fibre length and the fibre orientation distribution. Fibres can either be placed in one direction, be arranged in a weave, or arranged in accordance with some continuous orientation distribution

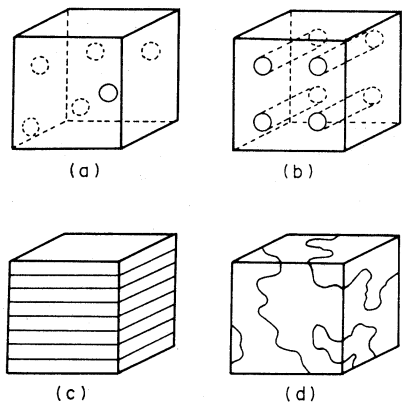

Figure 1: *a) particle composites, b) fibre composites, c) laminate composites and d) composites with irregular geometry.*

function. Fibre materials commonly used here are glass, carbon, aramid and wood. The surrounding phase, or matrix, is often some polymer such as epoxy or polyester.

1.3 Wood composite materials

Natural composite materials containing fibres or particles obtained from wood or from plants such as flax and hemp are gaining in popularity, both of environmental reasons and due to their high performance and their low cost and low weight. Wood-based composites are commonly created either by joining wood particles by some adhesive, by mixing wood flour with a thermoplastic [33] or by impregnating paper with a resin. An advantage of wood composites as compared with solid wood is that they are more homogenous and are without such weaknesses as knots. Such engineering wood products as glulam and laminated veneer lumber, on the other hand, are not considered as composite materials, whereas paper and fibre boards, which have a very low matrix phase volume fraction, sometimes are referred to as being composite materials.

High pressure laminates, or HPL, are wood fibre composites which have undergone a strong development during the last decade or so. They are composed of layers of craft paper impregnated with phenolic or melamine resin and cured under high pressure and at high temperature [3]. Although consisting of layers of differing stiffness, HPL is considered here as a fibre composite and not as a laminate composite. One problem in connection both with HPL and with all other wood composites, is that of shape instability when changes in moisture

content occur. This makes it important to have a good understanding of how to predict and control the stiffness and hygroexpansion properties of HPL.

2 Elastic Properties of Composite Materials

2.1 Homogenisation

Composite materials have gained in popularity in various industrial applications such as in the automotive, the space and the building industries. In all applications there is a need of simulating the mechanical behaviour of elements or of entire structures. Although computer simulation capacity is increasing, it will hardly be possible to model every single fibre, such as in an airplane for example. The only practical approach to simulation is to regard a composite material as being continuous and homogeneous. Since micro-scale properties such as fibre stiffness and orientation are decisive for the global behaviour of the material, homogenisation is very important.

Homogenisation also allowes one to calculate such effective properties as those of stiffness and hygroexpansion when the corresponding properties of the constituents as well as information concerning the geometry of the material, such as the direction in which the fibres are aligned, are known [34, 29]. A number of assumptions need to be made: that no chemical interaction between the different phases occurs, that the phases are homogeneous and distinctly separated, and that there is statistical homogeneity allowing one to define a volume element which is representative of the structure as a whole. In order to calculate the stiffness and the hygroexpansion of a composite made up of two linear elastic materials, one needs information on the stiffness matrices of the constituents, $\mathbf{D}_f$ and $\mathbf{D}_m$, the hygroexpansion coefficients vectors, $\boldsymbol{\beta}_f$ and $\boldsymbol{\beta}_m$, the volume fractions, V_f and V_m, and the shape as well as the orientation distribution of the fibres or particles.

Homogenisation is achieved by analysing a representative volume element, RVE. In its structure and composition the RVE is typical for the composite as a whole. Effective mechanical properties are calculated from the response of the RVE when exposed to a prescribed boundary force or deformation. When the effective hygroexpansion coefficients of the composites are calculated, which is done in a way directly analogous to calculation of the thermal expansion coefficients, the prescribed boundary conditions can be obtained by use of a prescribed change in moisture content.

The choice of boundary conditions influences the results, for example, when a

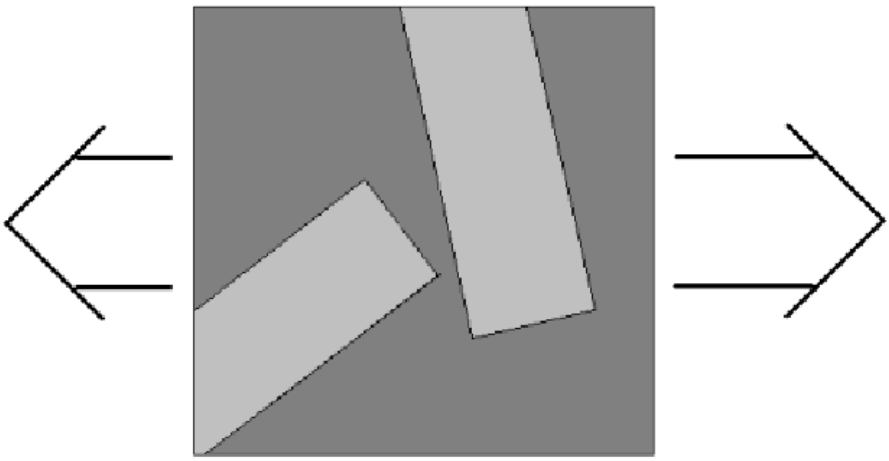

Figure 2: *A RVE exposed to a force in one direction.*

prescribed displacement at the boundary is assumed, the stiffness of the RVE is overestimated, due to the extra constraint. The assumption of a prescribed traction also results in the stiffness being underestimated. There is the possibility of using cyclic boundary conditions [20]. This requires use of a periodic geometry for the RVE, such as that of a fibre that passes through a boundary having the same inclination on the opposite side.

3 Literature Concerning Homogenisation Methods

Use of adequate methods for homogenisation is very important in simulating structures made of composite materials, since an error in the properties of the composite material results in an equally large error in the structural simulation, irrespective of how accurate the simulation may be. The greatest difficulty in homogenising materials is often that of obtaining reliable material data. For wood particles, there are nine stiffness components and three hygroexpansion components that need to be known or be estimated. If the properties of the constituents are known, it is the quality of the homogenisation model which

is decisive for the accuracy and reliability of predicting the properties of the composite material.

In working with composite homogenisation models, one is in good company, the first contributions to this research area having been made in the late 19th century by such scientists as Maxwell, Boltzmann and Einstein [34]. The most important and general models are the Voigt approximation (1889) [1] and the Reuss approximation (1929) [1], based on the assumption of homogeneous strain and of homogeneous stress, respectively. Hill (1952) [22], who showed that these two approximations are in fact boundaries for the overall stiffness components regardless of the geometry of the constituents, formulated a number of fundamental theoretical principles here [21]. The development of mathematical and, to various degrees, empirical models increased in the early 1960s when the technical importance of composite materials came clear.

Models for unidirectional fibre composites were created, such as the Halpin-Tsai equations (1963) [14] which are probably those most frequently employed. A number of methods for calculating transverse stiffness of composites containing fibres of differing geometries, such as the method of Hashin-Shtrikman bounds (1965) [17, 18], were derived.

Models for particle composites are usually derived by considering a single particle in an effective medium of some sort. Models of this type include the Eshelby equivalent inclusion method (1957) [11] for elliptical particles, the Mori-Tanaka theory (1973) [31], the self-consistent scheme (1965) and the generalized self-consistent scheme [15]. All existing models for particle composites assume the particles to be isotropic. A directional average for the particle phases can also be obtained, however without any great difficulty. Other approaches to the analysis of effective stiffness have been developed by Hashin [19, 16], Luciano [28] and Chen [7]. Theoretical analyse of the effect of the length and the orientation of the fibre have been carried out by Fu *et al.* [12], Sayers [37], Munson-McGee *et al.* [32] and Dunn *et al.* [10]. Stresses in the fibres and in the matrix have been investigated by Carman *et al.* [6].

Homogenisation of the hygroexpansion properties, which in mathematical terms is identical with thermal expansion, has become of lesser interest. Certain fundamental results for anisotropic composites have been derived by Levin [27], and by Rosen and Hashin [36, 19]. Camacho *et al.* [5] have performed 3D modelling and compared the results with measurement data.

Comprehensive reviews of composite material modelling are provided by Dunn

et al. [10] who present a long list of additional references; by Tucker [40] who compares a number of analytical models for unidirectional short fibre composites involving finite element calculations; and by Hashin [15], whose review is best, containing a very informative and critical review of the field of composite material analysis as a whole.

It would appear that most models concern rather specialized cases, such as those of isotropy, of long unidirectional fibres, or of circular or hexagonal fibre geometries, the one as accurate as the other. Most models provide estimates of elastic, transverse and longitudinal moduli [26]. Obviously, a great deal of work needs to be done to investigate more complicated composites such as those with anisotropic constituents or with fibre-to-fibre interactions, or that are non-unidirectional, such as HPL.

Models used in many industrial applications, such as the Halpin-Tsai equations or the rule of mixture, often suffice for estimating single effective properties such as longitudinal stiffness, but tend to be inadequate or inappropriate for estimating the other stiffness and hygroexpansion components needed, such as for the indata in the case of finite element analysis.

4 Models of Stiffness

4.1 The Voigt and the Reuss models

The simplest forms of homogenisation involve assuming either that the strain field or the stress field is uniform. The first of these two assumptions requiers adding the stresses weighted by the respective volume fractions, V_i, which yields to the expression for composite material stiffness matrices

$$\mathbf{D}^* = V_1\mathbf{D}_1 + V_2\mathbf{D}_2 \tag{1}$$

that Voigt [1] introduced, called the Voigt approximation or the rule of mixture, ROM. The asterisk indicates the effective property to be intended. Other designations of this approach, which is probably the homogenisation method most frequently employed, are the parallel coupling model and the homogeneous strain model. The assumption of a uniform strain field entails the tractions at the phase boundaries not being in equilibrium.

The approximation given by the assumption of a homogeneous stress field was introduced by Reuss [1]. It leads to the analogous expression

$$\mathbf{C}^* = V_1\mathbf{C}_1 + V_2\mathbf{C}_2 \tag{2}$$

where $\mathbf{C} = \mathbf{D}^{-1}$ is the compliance matrix. This is called the Reuss approximation or the series-coupling model. The strains under uniform stress are such that the deformations of the inclusions and the matrix are not compatible. The Voigt and the Reuss approximations are the most important ones since they constitute the bounds for all of the components in $\mathbf{D}^*$ of any composite material, regardless of its geometry, as determined by Hill [22] on the basis of rigorous calculations. These bounds are very easy to use, but if the properties of the constituents differ too much the provide too large an interval to be of practical use.

4.2 Interpolation between the Voigt and Reuss models

The one dimensional versions of parallel and of serial coupling can be written as a single equation with a parameter α [24] for a scalar stiffness parameter,

$$E^* = (V_1E_1^\alpha + V_2E_2^\alpha)^{1/\alpha} \tag{3}$$

where $\alpha = 1$ is the case of one-dimensional parallel coupling and $\alpha = -1$ that of the serial coupling. By giving the variable α a particular value $-1 < \alpha < 1$ an interpolation is achieved. For $\alpha = 0$ the equation can be written as $E^* = V_1^{E_1} \cdot V_2^{E_2}$. Observe that $\alpha = 1$ corresponds to the arithmetic mean, $\alpha = -1$ to the harmonic mean and $\alpha = 0$ to the geometric mean of the stiffnesses.

This interpolation can also be extended to the two- and three dimensional case, as shown by Stålne [38]

$$\mathbf{D}^* = (V_1\mathbf{D}_1^\alpha + V_2\mathbf{D}_2^\alpha)^{1/\alpha} \tag{4}$$

The interpolation can be performed on an integral as well, as will be shown in the section "Composites containing arbitrarily oriented fibres".

4.3 The self-consistent scheme

The self-consistent scheme can be used to estimate the effective bulk and shear moduli of particle composites containing isotropic constituents. The general idea is here to consider a single spherical isotropic particle embedded in an infinite isotropic effective medium, see Figure 3. The state of strain in one particle is assumed to not be affected by the state of strain in another.

Figure 3: *Self-consistent scheme, sphere in an effective medium.*

The unknown properties of the effective medium, of the effective bulk modulus K^*, and of the effective shear modulus G^* can be approximated by use of the equations

$$\begin{aligned} \frac{V_1}{K^* - K_2} + \frac{V_2}{K^* - K_1} &= \frac{3}{3K^* + G^*} \\ \frac{V_1}{G^* - G_2} + \frac{V_2}{G^* - G_1} &= \frac{6(K^* + 2G^*)}{5G^*(3K^* + 4G^*)} \end{aligned} \tag{5}$$

as given by Hill [23]. It should be noted that when the particle phase is stiffer than the matrix material, which is the usual case since one generally wants to reinforce the matrix, this model overestimates the effective moduli [15].

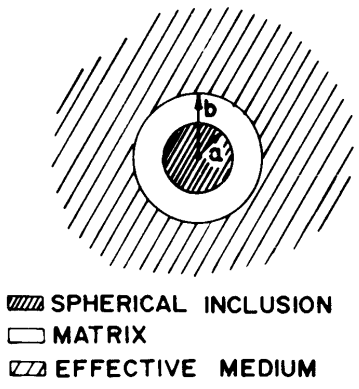

Figure 4: *Generalised self-consistent scheme, sphere with a concentric shell of matrix material in an effective medium.*

A generalised version of this self-consistent scheme involves a concentric shell

of matrix material surrounding the spherical particle, Figure 4. This version is considered more realistic, but is also far more complicated and has no explicit solution.

4.4 The Halpin-Tsai equations

The most popular model for predicting the stiffness of short unidirectional fibre composites is that involving the Halpin-Tsai equations [14]. These were derived from approximations of Hill's generalised self-consistent model [23]. In dealing with the composite, each fibre is assumed to behave as though it were surrounded by a pure matrix cylinder, a body with the properties of the composite lying outside the cylinder. The constituents are considered to be homogeneous and to be transversely isotropic in the direction of the fibre. The composite stiffness in the longitudinal direction is given by

$$\begin{aligned} E_L^* &= E_m \frac{1 + \xi\eta V_f}{1 - \eta V_f} \\ \eta &= \frac{E_f - E_m}{E_f + \xi E_m} \end{aligned} \tag{6}$$

where E_m is the matrix material stiffness and $\xi = 2a/b$ is a factor of the geometry controlled by the fibre length-thickness ratio a/b, where a is the fibre length and b the fibre thickness as shown in Figure 5.

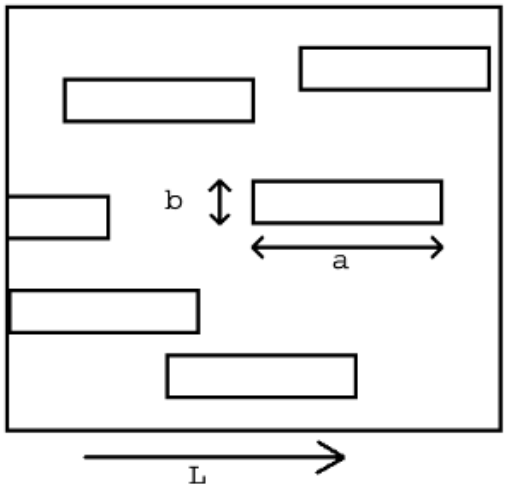

Figure 5: *Fibres of length a and width b in a matrix material.*

The Halpin-Tsai equations represent an interpolation between one-dimensional parallel coupling and serial coupling, observable when the cases of $\xi = 0$ and $\xi \to \infty$ are studied,

$$\begin{aligned} \lim_{\xi \to \infty} E_L^* &= V_f E_f + (1 - V_f) E_m \\ E_L^*(\xi = 0) &= \left(\frac{V_f}{E_f} + \frac{(1 - V_f)}{E_m} \right)^{-1} \end{aligned} \tag{7}$$

Although this is universally accepted as a model for longitudinal stiffness, its use for obtaining transverse stiffness, E_T, for $\xi = 2$ as the authors suggests, or for obtaining ν_L or G_L, is not recomended by Hashin [15]. The Halpin-Tsai equations are best used for low fibre concentrations since at higher concentrations they overestimate the effective stiffness.

4.5 The Hashin-Shtrikman bounds

The Hashin-Shtrikman bounds [17, 18] are one of the best known types of bounds, next to the Reuss-Voigt bounds. The most general form of them is that for isotropic 3D multiphase mixtures of arbitrary phase geometry, although they are most commonly used for estimating the plane strain bulk modulus, $\overline{k} = 1/2\ (D_{11} + D_{12})$, and the transverse shear modulus, $\overline{\mu} = 1/2\ (D_{11} - D_{12})$, of a transversely isotropic two-phase composite. Plane strain means that the longitudinal displacement is zero, the longitudinal direction here being the 3-direction. The moduli must satisfy

$$\begin{aligned} k_l \leq \overline{k} \leq k_u \\ \mu_l \leq \overline{\mu} \leq \mu_u \end{aligned} \tag{8}$$

where

$$\begin{aligned} k_l &= k_2 + \frac{V_1}{\frac{1}{k_1 - k_2} + \frac{V_2}{k_2 + \mu_2}}, \\ k_u &= k_1 + \frac{V_2}{\frac{1}{k_2 - k_1} + \frac{V_1}{k_1 + \mu_1}}, \\ \mu_l &= \mu_2 + \frac{V_1}{\frac{1}{\mu_1 - \mu_2} + \frac{V_2 (k_2 + 2\mu_2)}{2\mu_2 (k_2 + \mu_2)}}, \\ \mu_u &= \mu_1 + \frac{V_2}{\frac{1}{\mu_2 - \mu_1} + \frac{V_1 (k_1 + 2\mu_1)}{2\mu_1 (k_1 + \mu_1)}} \end{aligned} \tag{9}$$

where V_i is the volume fraction of the material i. This provides a rather narrow interval for the effective properties that are estimated. The Hashin-Shtrikman

bounds are often used when other models are compared. They can also be used for example, for determining the bounds for fitting parameters of models such as the Halpin-Tsai equations [41].

4.6 Composites containing arbitrarily oriented fibres

In engineering applications involving fibres with an orientation distribution, such as planar random distribution or a distribution in terms of some distribution function, use is often made of laminate theory. This is equivalent to the Voigt approximation which is regarded as being closer to the correct effective properties than the Reuss approximation is. The procedure [38] employed is to calculate the properties of a unidirectional fibre composite and to integrate all contributions from each of the infinitesimal angular interval

$$\mathbf{D}^* = \int_0^\pi \mathbf{D}_c f(\varphi)\, d\varphi \tag{10}$$

where $f(\varphi)$ is a planar fibre orientation distribution function with the angle φ to the x-axis and $\mathbf{D}_c$ is the stiffness matrix of the unidirectional fibre composite transformed into global coordinates. For the case of ramdomly oriented fibres $f(\varphi) = \frac{1}{\pi}$. This equation can be transformed into one for three dimensions for estimating composites with a spatial fibre orientation distribution

$$\mathbf{D}^* = \int_0^\pi \int_0^\pi \mathbf{D}_c \psi(\varphi, \theta) \sin\theta \, d\varphi d\theta \tag{11}$$

where $\psi(\varphi, \theta) = \frac{1}{2\pi}$ in the case of statistical isotropy, θ is the angle between the fibre and the z-axis and φ is the angle between the fibres projection in the $x - y$ plane with the x-axis, which is normally termed a spherical coordinate system. This implies that the fibres are transversely isotropic, or at least statistically transversely isotropic. This choice of an angular definition is employed, for example in [5, 12, 38]. Another common way of representing the coordinate transformation is by use of the Euler angles, as in [10, 32, 37]. These are the three angles between the i-th global coordinate axis and the i-th axis in the fibre coordinate system.

Practically all integrations found in the literature are performed with use of the homogeneous strain assumption, $\mathbf{D}$-matrices being added of small intervals. Although this overestimates the effective stiffness, the interpolation described earlier can also be used here:

$$\mathbf{D}^* = \left[\int_0^\pi \int_0^\pi \mathbf{D}_c^\alpha \psi(\varphi, \theta) \sin\theta \, d\varphi d\theta \right]^{1/\alpha} \tag{12}$$

where $-1 \leq \alpha \leq 1$ as stated previously.

A simple and quick way of calculating the isotropic stiffness and the isotropic shear rigidity of a planar random composite by use of laminate theory [39] is through employing the approximation

$$\begin{aligned} E^* &= \frac{3}{8}E_{11} + \frac{5}{8}E_{22} \\ G^* &= \frac{1}{8}E_{11} + \frac{1}{4}E_{22} \end{aligned} \tag{13}$$

where E_{11} is the stiffness of the unidirectional lamina in the fibre direction and E_{22} is the stiffness of them in the transverse direction (E_{11} must be greater than E_{22}). The greater the difference between the moduli is, the more accurate the expression becomes.

For fibrous materials such as paper, Cox's classic model [8] is sometimes employed. It assumes only the longitudinal stiffness, E_f, of the fibres and a state of homogeneous strain. For an isotropic fibre distribution, Young's modulus and Poisson's ratio become

$$\begin{aligned} E^* &= \frac{1}{3}V_f E_f \\ \nu^* &= \frac{1}{3} \end{aligned} \tag{14}$$

where V_f is the volume density of the fibre material. This model is not recommended for estimating the properties of multiphase materials, however, since it neglects the influence of the transverse stiffness and the shear stiffness of the fibres.

5 Models of Hygroexpansions

An equation for the effective hygroexpansion coefficients of a general 2-phase material or for the thermal expansion coefficients, since from a mathematical point of view the problem envolved is identical, was derived by Levin [27]. It was extended by Rosen and Hashin [36] to generally anisotropic 2-phase composites and to an arbitrary phase geometry in the form

$$\boldsymbol{\beta}^* = \boldsymbol{\beta}^{(1)} + (\boldsymbol{\beta}^{(2)} - \boldsymbol{\beta}^{(1)})(\mathbf{C}^{(2)} - \mathbf{C}^{(1)})^{-1}(\mathbf{C}^* - \mathbf{C}^{(1)}) \tag{15}$$

where $\boldsymbol{\beta}^*$ and $\mathbf{C}^*$ are the effective hygroexpansion coefficients and the effective compliance tensor, respectively. $\boldsymbol{\beta}^{(i)}$ and $\mathbf{C}^{(i)}$, in turn, are the hygroexpansion

coefficients and the compliance tensors of the phases, respectively. For statistically isotropic composites with isotropic phases, the equation simplifies to

$$\beta^* = \beta^{(1)} + \frac{\beta^{(2)} - \beta^{(1)}}{1/K_2 - 1/K_1}(1/K^* - 1/K_1) \tag{16}$$

where K^* is the effective bulk modulus and K_1 and K_2 are the phase bulk moduli. In the case of a transversely isotropic fibre composite with isotropic fibre and matrix phases, the hygroexpansion components become

$$\begin{aligned} \beta_L^* &= \beta^{(1)} + \frac{\beta^{(2)} - \beta^{(1)}}{1/K_2 - 1/K_1}\left[\frac{3(1-2\nu_L^*)}{E_L^*} - \frac{1}{K_1}\right] \\ \beta_T^* &= \beta^{(1)} + \frac{\beta^{(2)} - \beta^{(1)}}{1/K_2 - 1/K_1}\left[\frac{3}{2k^*} - \frac{3(1-2\nu_L^*)}{E_L^*} - \frac{1}{K_1}\right] \end{aligned} \tag{17}$$

where k^* is the effective transverse bulk modulus. In [36] a corresponding equation for the general multiphase effective hygroexpansion is also given.

An interesting conclusion to be drawn from equation (15) is that the hygroexpansion components follow from the effective stiffnesses without further approximations being required. The bounds for the hygroexpansion coefficients can be obtained by calculating the bounds for stiffnesses and then calculating the corresponding hygroexpansion.

For a composite like that represented in the HPL equation (15), however, is only applicable at the first step in the homogenisation of a single fibre in a matrix material inclusion, rather than for an entire fibre network. For a network made up of fibres contained in inclusions, the hygroexpansion can be calculated in accordance with the homogeneous strain assumption

$$\boldsymbol{\varepsilon}^* = \int_0^\pi \int_0^\pi \mathbf{D}^{*-1}\mathbf{D}\,\boldsymbol{\varepsilon}^o \psi(\varphi,\theta)\sin\theta\, d\varphi d\theta \tag{18}$$

where $\mathbf{D}$ is the stiffness matrix of a homogenised unidirectional fiber composite at an angle that is transformed into that of the global coordinate system, and $\boldsymbol{\varepsilon}^o$ is the free hygroexpansion of the same composite.

6 Stiffness calculation of a HPL

The following illustrates calculation of the stiffness of a core layer (phenolic resin impregnated paper) of a high-pressure laminate. The stiffness properties of the constituents are taken from [35] which concerns the properties of a single wood fibre, and from [4], which deals with the stiffness properties of a phenolic resin.

Table 1: *Elastic properties of wood fibres and of phenolic resin.*

Fibre						Matrix	
E_x	$E_y = E_z$	$\nu_{xy} = \nu_{xz}$	ν_{yz}	$G_{xy} = G_{xz}$	G_{yz}	E	ν
[MPa]	[MPa]	[-]	[-]	[MPa]	[MPa]	[MPa]	[-]
40 000	5 000	0.2	0.3	4 000	1 920	5 750	0.3

The stiffness of melamine resin is given in [13]. The stiffness in the x-direction, which is the machine direction in which the greatest number of fibres is aligned, and in the y-direction, which is the cross direction, is plotted as a function of the fibre volume fraction. In both diagrams the solid lines are the Voigt and the Reuss bounds, representing the maximum and minimum, respectively, of the possible stiffnesses. This assumes, of course, that the indata in table 1 are correct. At a high fibre volume fraction, one of 75 %, there is a large gap between the bounds.

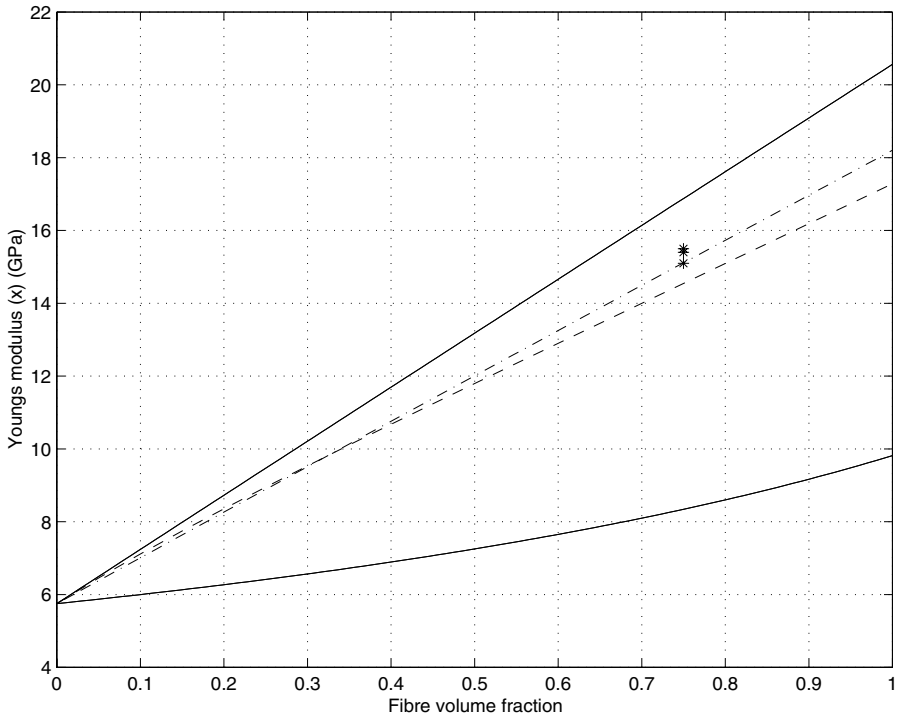

Figure 6: *Solid lines = the Voigt and Reuss bounds, dashed = Stålne-Gustafsson model, dashed-dotted = isotropic Voigt. The stars represent the measurement of HPL in the x-direction.*

The dash-dotted lines in both diagrams are from simple calculations made un-

der the assumption of a homogeneous state of strain (Voigt) and of an isotropic (random) fibre orientation distribution. This appears to agree with the measurements made in the stiffer x-direction [2], whereas it clearly overestimates the stiffness in the weaker y-direction, since the model predicts the same stiffness in both directions.

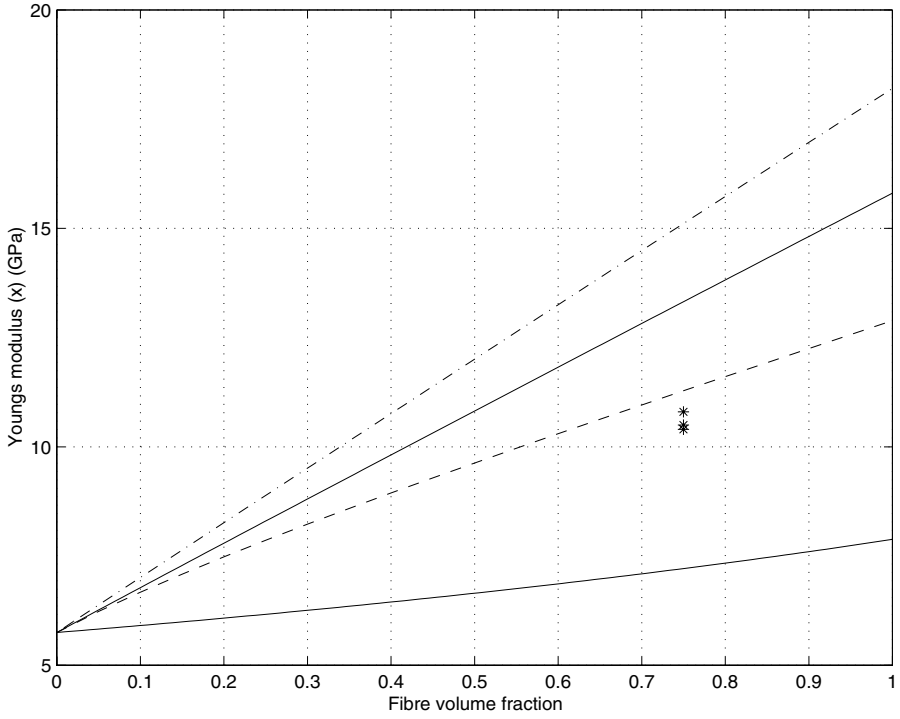

Figure 7: *Solid lines = the Voigt and Reuss bounds, dashed = Stålne-Gustafsson model, dashed-dotted = isotropic Voigt. The stars represent the measurement of HPL in the y-direction.*

The dashed lines are calculations from a model created by Stålne and Gustafsson, described in [38], with a fibre orientation distribution involving 1.8 times as many fibres in the x-direction as in the y-direction, and with an interpolation between the Voigt and the Reuss bounds. The model appears to underestimate the stiffness in the x-direction but to overestimate the stiffness in the y-direction. This suggests the figure of 1.8 given by the HPL manufacturer to be too low, the HPL in fact having more fibres in the x-direction than the manufacturer indicates.

References

[1] Aboudi, J. (1991). *Mechanics of Composite Materials*, Elsevier, Amsterdam, The Netherlands, 14-18.

[2] Andersson, B. (1999). *Composite materials' hygro-mechanical properties*, Masters thesis, Report TVSM-3018, Div. of Structural Mechanics, Lund University, Sweden.

[3] Adl Zarrabi, B. (1998). *Hygro-Elastic Deformation of High Pressure Laminates*, Doctoral thesis, Div. of Building Material, Chalmers University of Technology, Göteborg, Sweden

[4] Barth, Th. (1984). "Der Einfluss der Feuchteaufnahme auf die mechanischen Eigenschaften von Phenolplasten." *Z. Werkstofftech*, Verlag Chemie, Weinheim, Germany, 15, 299-308.

[5] Camacho, C.W., Tucker, C.L. (1990). "Stiffness and Thermal Expansion Predictions for Hybrid Short Fiber Composites". *Polymer Composites*, 11, 229-239.

[6] Carman, G.P., Reifsnider, K.L. (1992). "Micromechanics of Short-Fiber Composites", *Composites Science and Technology*, 43, 137-146.

[7] Chen, H.-J., Tsai, S.W. (1996). "Three-Dimensional Effective Moduli of Symmetric Laminates". *Journal of Composite Materials*, 30, 906-917.

[8] Cox, H.L. (1951). "The elasticity and strength of paper and other fibrous materials." *Brittish Journal of Applied Physics*, 3, 72-79.

[9] Dinwoodie, J.M. (1989). *Wood: nature's cellular, polymeric fibre-composite*, The Institute of Metals, London, 57. Dinwoodie – Wood: nature's cellular, polymeric fibre-composite : Trsiffror

[10] Dunn, M. L., Ledbetter, H., Heyliger, P. R. and Choi, C. S. (1996). "Elastic constants of textured short-fiber composites." *J. Mech. Phys. Solids*, Elsevier, Amsterdam, The Netherlands, 44, 1509-1541.

[11] Eshelby, J.D, (1957). "The determination of the field of an elliptical inclusion and related problems", *Proceedings of the Royal Society*, London, Vol A, No. 241, p 376-396.

[12] Fu, S.-Y. Lauke, B. (1998). "An analytical characterization of the anisotropy of the elastic modulus of misaligned short-fiber-reinforced polymers." *Composites Science and Technology*, 58, 1961-1972.

[13] Hagstrand, P.-O. *Mechanical Analysis of Melamine-Formaldehyde Composites*, Doctoral thesis, Dept. of Polymeric Material, Chalmers University of Technology, Göteborg, Sweden.

[14] Halpin, J.C., Kardos, J.L. (1976). "The Halpin-Tsai equations: A review." *Polymer Engineering and Science*, 16, 344-352.

[15] Hashin, Z. (1983) "Analysis of Composite Materials, A Survey", *Journal of Applied Mechanics*, 9, 481-505.

[16] Hashin, Z. (1979) "Analysis of Properties of Fiber Composites with Anisotropic Constituents" *Journal of Applied Mechanics*, 46, 543-550.

[17] Hashin, Z., Shtrikman, S. (1963). "A variational approach to the theory of the elastic behaviour of multiphased materials." *J. Mech. Phys. Solids*, 11, 127-140.

[18] Hashin, Z. (1965). "On Elastic Behaviour of Fibre Reinforced Materials of Arbitrary Transverse Phase Geometry". *Journal of the Mechanics and Physics of Solids*, 13, 119-134.

[19] Hashin, Z., Rosen, B.W. (1964). "The Elastic Moduli of Fiber-Reinforced Materials". *Journal of Applied Mechanics*, 6, 223-232.

[20] Heyden, S. (2000). *Network modelling for the evaluation of mechanical properties of cellulose fibre fluff.*, Doctoral thesis, Report TVSM-1011, Div. of Structural Mechanics, Lund University, Sweden.

[21] Hill, R. (1963) "Elastic Properties of Reinforced Solids: Some Theoretical Principals". *Journal of the Mechanics and Physics of Solids*, 11, 357-372.

[22] Hill, R. (1952) "Elastic Behaviour of a Crystalline Aggregate". *Proceedings of the Physical Society*, Section A, 349-354.

[23] Hill, R. (1965) "A Self Consistent Mechanics of Composite Materials". *Journal of the Mechanics and Physics of Solids*, 13, 213-222.

[24] Hillerborg, A. (1986). *Kompendium i Byggnadsmateriallära FK*, Division of Building Materials, Lund University, Sweden.

[25] Hult, J., Bjarnehed, H. (1993). *Styvhet och Styrka - Grundläggande Kompositmekanik*, Studentlitteratur, Lund, Sweden.

[26] Ju, J.W., Zhang, X.D. (1998). "Micromechanics and Effective Transverse Elastic Moduli of Composites with Randomly Located Aligned Circular Fibers". *International Journal of Solids and Structures*, 35, 941-960.

[27] Levin, V.M. (1967). "On the Coefficients of Thermal Expansion of Heterogeous Materials". *Mechanics of Solids*, 2, 58-61.

[28] Luciano, R., Barbero, E.J. (1994). "Formulas for the Stiffness of Composites with Periodic Microstructure". *International Journal of Solids and Structures*, 31, 2933-2944.

[29] Lukkassen, D., Persson, L.-E., Wall, P. (1994). *Some Engineering and Mathematical Aspects on the Homogenization Method for Computing Effective Moduli and Microstresses in Elastic Composite Materials*, Research Report 2, Dept. of Mathematics, Luleå University of Technology, Sweden.

[30] Moavenzadeh, F. (1990). *Concise Encyclopedia of Building and Construction Materials*, New York, USA.

[31] Mori, T., Tanaka, K. (1973) "Average Stress in Matrix and Average Elastic Energy of Materials with Misfitting Inclusions". *Acta Metallurgica*, 21, 571-574.

[32] Munson-McGee, S.H., McCullough, R.L. (1994). "Orientation Parameters for the Specification of Effective Properties of Heterogeneous Materials". *Polymer Engineering and Science*, 34, 361-370.

[33] Oksman, K. (1997). *Improved Properties of Thermoplastic Wood Flour Coumposites*, Doctoral thesis, 1997-17, Div. of Wood Technology, Luleå University of Technology, Sweden.

[34] Persson, L.E., Persson, L., Svanstedt, N., Wyller, J. (1993) *The Homogenization Method*, Studentlitteratur, Lund, Sweden.

[35] Persson, K. (1997). *Modelling of wood properties by a micromechanical approach.*, Licentiate thesis, Report TVSM-3018, Div. of Structural Mechanics, Lund University, Sweden.

[36] Rosen, B.W., Hashin, Z. (1970) "Effective Thermal Expansion Coefficients and Specific Heats of Composite Materials", *Inernational Journal of Engineering Science*, 8, 157-173.

[37] Sayers, C.M. (1992). "Elastic anisotropy of short-fibre reinforced composites." *International Journal of Solids and Structures*, 29, 2933-2944.

[38] Stålne, K., Gustafsson, P.J. (2000). "A 3D Model for Analysis of Stiffness and Hygroexpansion Properties of Fibre Composite Materials", *Journal of Engineering Mechanics*, in press.

[39] Tsai, S.W., Pagano, N.J. (1968). "Invariant Properties of Composite Materials" *Composite Materials Workshop*, Technomic Publishing Co. Stamford, Connecticut, 233-253.

[40] Tucker, C.L., Liang, E. (1999). "Stiffness Predictions for Unidirectional Short-Fiber Composites: Review and Evaluation" *Composites Science and Technology* 59, 655-671.

[41] Wall, P. (1994). *A Comparison of Homogenization, Hashin-Shtrikman Bounds and the Halpin-Tsai Equations*, Research Report 21, Dept. of Mathematics, Luleå University of Technology, Sweden.

II

Analysis of Fibre Composite Models for Stiffness and Hygroexpansion

Kristian Stålne
Division of Structural Mechanics
Lund University, Sweden

Abstract

In this report analytical models for elastic properties and hygroexpansion of fibre composite materials are presented. The cases of homogeneous strain and homogeneous stress are studied for 2D and 3D states of stress. There is also an interpolation between the two cases and it is shown that the interpolation is unambiguous and fulfills the coordinate invariance principle.

Keywords

Micromechanical model, mechanical properties, composite material, stiffness, hygro expansion.

Förord

This is the first report produced in the research project "Composite Material Moisture Mechanics" financed by the research collegue " Wood Mechanics".
I would like to thank my supervisor Per Johan Gustafsson for help and encouragement.

Kristian Stålne

Lund, September 1999

Sammanfattning

I rapporten presenteras analytiska modeller för styvhet och hygroexpansion för fiberkompositmaterial. Modellerna utgår från fallen homogent töjningstillstånd respektive homogent spänningstillstånd och kan tillämpas i både två och tre dimensioner. Vidare föreslås en interpolation mellan de båda extremfallen och det visas att denna är entydig och koordinatinvariant.

Innehåll

1 Introduction

The usage of fibre composite materials is today increasing in different applications in order to combine stiffness and strength with low weight. This leads to a greater need of models for prediction of the properties and behaviour of the composite material from the constituents properties. There are many different homogenisations and network mechanics models in use today [1, 2, 3]. The most dominating in this case is probably the Halpin-Tsai equations [4] which has been used frequently since the 60s , mostly for short fibre composites.

The models discussed here shows different alternatives when computing the stiffness matrix and hygroexpansion of a composite material. Indata to the calculation of stiffness is the stiffness matrices of the constituting material componetns, volume fractions and orientation distribution of the fibres. The hygroexpansion of the composite is estimated in a similair way from the constituents free hygroexpansions. The results contains bounds for stiffness and hygroexpansion and an interpolation between the extreme cases according to a generalisation using the method of weighted potence means.

This report contains coordinate transformations for stresses, strains and stiffness matrices, followed by a summation of stiffness matrices and an integration over all fibres. Then the hygroexpansion is taken into account after which the interpolation model is presented for the case of plane stress. Using matrix theory and an alternative definition of the stress and strain vectors the model is shown to be coordinate invariant. Finally the model is generalised to three dimensions.

2 Transformation of stresses and strains

When a coordinate system is rotated the angle φ are the stresses transformed at the state of plane stress according to [5]

$$\begin{aligned} \sigma_x &= \sigma_X \cos^2\varphi + \sigma_Y \sin^2\varphi + 2\tau_{XY}\sin\varphi\cos\varphi \\ \sigma_y &= \sigma_X \sin^2\varphi + \sigma_Y \cos^2\varphi - 2\tau_{XY}\sin\varphi\cos\varphi \\ \tau_x &= -\sigma_X \sin\varphi\cos\varphi + \sigma_Y \sin\varphi\cos\varphi + \tau_{XY}(\cos^2\varphi - \sin^2\varphi) \end{aligned} \tag{1}$$

where x-y are local coordinates and X-Y are global coordinates.

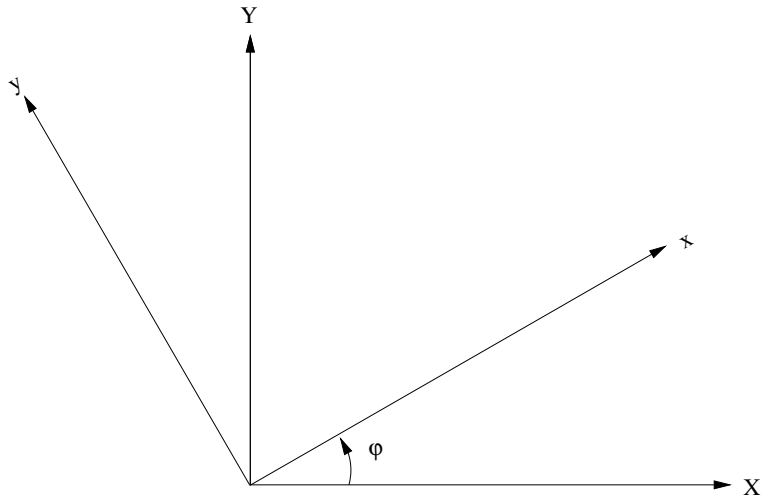

Figur 1: *Rotation of the coordinate system with the angle φ from the global (X-Y) to the fibres coordinate system x-y.*

This can be written in matrix notation as

$$\begin{bmatrix} \sigma_x \\ \sigma_y \\ \tau_{xy} \end{bmatrix} = \begin{bmatrix} m^2 & n^2 & 2mn \\ n^2 & m^2 & -2mn \\ -mn & mn & m^2 - n^2 \end{bmatrix} \begin{bmatrix} \sigma_X \\ \sigma_Y \\ \tau_{XY} \end{bmatrix} \tag{2}$$

with $m = \cos\varphi$ and $n = \sin\varphi$. This can be written as

$$\overline{\boldsymbol{\sigma}} = \mathbf{T}\boldsymbol{\sigma} \tag{3}$$

From here on an overline ($\overline{\boldsymbol{\sigma}}$, $\overline{\boldsymbol{\epsilon}}$) indicates local stress and strain etc.

Same transformation rules applies for the strain as well

$$\begin{bmatrix} \epsilon_x \\ \epsilon_y \\ \epsilon_{xy} \end{bmatrix} = \begin{bmatrix} m^2 & n^2 & 2mn \\ n^2 & m^2 & -2mn \\ -mn & mn & m^2 - n^2 \end{bmatrix} \begin{bmatrix} \epsilon_X \\ \epsilon_Y \\ \epsilon_{XY} \end{bmatrix} \tag{4}$$

Observe that $\epsilon_{xy} = \frac{1}{2}\gamma_{xy}$ and that $\epsilon_{XY} = \frac{1}{2}\gamma_{XY}$. If the shear strain is expressed with γ_{XY} the transformation matrix has to be changed to

$$\begin{bmatrix} \epsilon_x \\ \epsilon_y \\ \gamma_{xy} \end{bmatrix} = \begin{bmatrix} m^2 & n^2 & mn \\ n^2 & m^2 & -mn \\ -2mn & 2mn & m^2 - n^2 \end{bmatrix} \begin{bmatrix} \epsilon_X \\ \epsilon_Y \\ \gamma_{XY} \end{bmatrix} \tag{5}$$

or in short notation

$$\overline{\boldsymbol{\epsilon}} = \mathbf{T}^{-T}\boldsymbol{\epsilon} \tag{6}$$

where $\mathbf{T}^{-T}$ is the inverse of the transpose of $\mathbf{T}$. The difference between transformation of stress and strain can be eliminated by using ϵ_{xy} instead of γ_{xy} and compensate for in the stiffness matrix by doubling element $\overline{Q_{44}}$. From now on $\boldsymbol{\epsilon} = \begin{bmatrix} \epsilon_X & \epsilon_Y & \gamma_{XY} \end{bmatrix}^T$. Observe that

$$\mathbf{T}^T \neq \mathbf{T}^{-1} \tag{7}$$

3 The stiffness matrix at homogeneous states

3.1 Fibre network at homogeneous state of strain

The fibres are considered as orthotropic discs with different orientaion. At homogeneous state of strain it is assumed that alla fibres have the same strain at all points. This is equivalent to laminate theory. The stiffness matrix, $\mathbf{D}$, can be calculated by summing of the transformation of each fibre stiffness matrix of each orientation. The consitutive equation $\overline{\boldsymbol{\sigma}} = \overline{\mathbf{D}}\overline{\boldsymbol{\epsilon}}$ for the fibre in the local coordinate system written with all components is

$$\overline{\boldsymbol{\sigma}} = \frac{1}{1-\nu_{xy}\nu_{yx}} \begin{bmatrix} E_x & \nu_{yx}E_x & 0 \\ \nu_{xy}E_y & E_y & 0 \\ 0 & 0 & (1-\nu_{xy}\nu_{yx})G_{xy} \end{bmatrix} \overline{\boldsymbol{\epsilon}} \tag{8}$$

This gives, with the transformation equation for stress and strain,

$$\boldsymbol{\sigma} = \mathbf{T}^{-1}\overline{\boldsymbol{\sigma}} = \mathbf{T}^{-1}\overline{\mathbf{D}}\overline{\boldsymbol{\epsilon}} = \mathbf{T}^{-1}\overline{\mathbf{D}}\mathbf{T}^{-T}\boldsymbol{\epsilon} \tag{9}$$

and the stiffness matrix can in the global coordinates be written as

$$\mathbf{D} = \mathbf{T}^{-1}\overline{\mathbf{D}}\mathbf{T}^{-T} \tag{10}$$

The resulting stiffness matrix of the entire fibre network is calculated by summing (integrating) all fibres.

$$\mathbf{D}_f = \int_0^{\pi} \mathbf{T}^{-1}\overline{\mathbf{D}}\mathbf{T}^{-T} \cdot f(\varphi) d\varphi \tag{11}$$

where $f(\varphi)$ is the fibre orientation distribution function which has the form $f(\varphi) = A + B\cos^2\varphi$ and is closer examined in section 6.2. For isotropic orientation distribution $f(\varphi) = \frac{1}{\pi}$ and for an orthotropic orientation distribution at 1:p, where p is how many times higher the fibre density is in the x-direction than in the y-direction, $f(\varphi)$ becomes

$$f(\varphi) = \frac{2}{\pi} \cdot \frac{1 + (p-1)cos^2\varphi}{p+1} \tag{12}$$

3.2 Fibre network at homogeneous state of stress

In this case the stress at all points is assumed to be equal and stiffness of the fibre network is achived by summing of all strains. In the case of homogeneous strain all stiffness matrices was summed, here all compliance matrices are summed, $\mathbf{S} = \mathbf{D}^{-1}$. According to the above

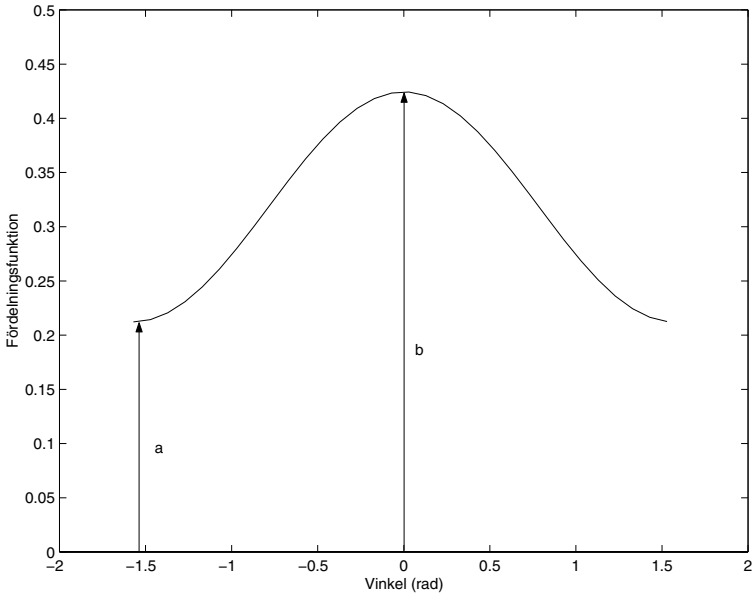

Figur 2: *Fibre orientation distribution function* $f(\varphi)$. $p = \frac{b}{a}$

$$\mathbf{D} = \mathbf{T}^{-1}\overline{\mathbf{D}}\mathbf{T}^{-T}$$

gives

$$\mathbf{S} = \mathbf{D}^{-1} = (\mathbf{T}^{-1}\overline{\mathbf{D}}\mathbf{T}^{-T})^{-1} = \mathbf{T}^{T}\overline{\mathbf{D}}^{-1}\mathbf{T} = \mathbf{T}^{T}\overline{\mathbf{S}}\mathbf{T} \tag{13}$$

Summarising all compliance matrices gives

$$\mathbf{S}_f = \int_0^{\pi} \mathbf{T}^{T}\overline{\mathbf{S}}\mathbf{T} \cdot f(\varphi)d\varphi \tag{14}$$

or

$$\mathbf{D}_f = \left[\int_0^\pi \mathbf{T}^T \overline{\mathbf{D}}^{-1} \mathbf{T} \cdot f(\varphi) d\varphi\right]^{-1} = \left[\int_0^\pi (\mathbf{T}^{-1} \overline{\mathbf{D}} \mathbf{T}^{-T})^{-1} \cdot f(\varphi) d\varphi\right]^{-1} \quad (15)$$

3.3 Stiffness matrices of composite materials with two phases

If another material is added to the fibre network, the components stiffness matrices can be summarised, weighted with the volume fractions respectively, in analogy with the integration

$$\mathbf{D}_c = V_m \mathbf{D}_m + V_f \mathbf{D}_f \quad (16)$$

according to the model of parallel coupling. That can also be done using the serial coupling model

$$\mathbf{D}_c = \left(V_m \mathbf{D}_m^{-1} + V_f \mathbf{D}_f^{-1}\right)^{-1} \quad (17)$$

4 Hygroexpansion

The free hygroexpansion of a fibre is denoted $\overline{\boldsymbol{\epsilon}}^0$ in the local coordinate system of the fibre and is defined

$$\overline{\boldsymbol{\epsilon}}^0 = \begin{bmatrix} \epsilon_L \\ \epsilon_T \\ 0 \end{bmatrix} = p(\xi) \begin{bmatrix} \epsilon_L(max) \\ \epsilon_T(max) \\ 0 \end{bmatrix} \tag{18}$$

where $p(\xi)$ is the relative strain as a function of the relative humidity, ξ, $\epsilon_L(max)$ and $\epsilon_T(max)$ are the hygroexpansion at saturated humidity [7].

4.1 Serial coupling

The simplest way of calculating the hygroexpansion of a composite material is the serial coupling model. The total strain is the sum of the strains of all components multiplied with the respective volume fractions

$$\boldsymbol{\epsilon}_c^0 = V_1\boldsymbol{\epsilon}_1^0 + V_2\boldsymbol{\epsilon}_2^0 \tag{19}$$

where $\boldsymbol{\epsilon}_1^0$ and $\boldsymbol{\epsilon}_2^0$ are the components free hygroexpansion strains. For k number of components the total strain is

$$\boldsymbol{\epsilon} = \sum_{i=1}^{k} V_i \boldsymbol{\epsilon}_i^0 \tag{20}$$

The corresponding integral for all fibre directions the total strain $\boldsymbol{\epsilon}_f^0$ of the fibre network becomes

$$\boldsymbol{\epsilon}_f^0 = \int_0^\pi \boldsymbol{\epsilon}^0 \cdot f(\varphi) d\varphi = \int_0^\pi \mathbf{T}^T \overline{\boldsymbol{\epsilon}}^0 \cdot f(\varphi) d\varphi \tag{21}$$

4.2 Parallel coupling

Parallel coupling means a homogeneous state of strain, which at a constrained hygroexpansion leads to the stress

$$\boldsymbol{\sigma} = V_1 \boldsymbol{\sigma}_1 + V_2 \boldsymbol{\sigma}_2 \tag{22}$$

where $\boldsymbol{\sigma}_1 = \mathbf{D}_1 \boldsymbol{\epsilon}_1^0$ and $\boldsymbol{\sigma}_2 = \mathbf{D}_2 \boldsymbol{\epsilon}_2^0$. This stress gives the free hygroexpansion strain

$$\boldsymbol{\epsilon}_c^0 = \mathbf{D}_c^{-1} \boldsymbol{\sigma} = V_1 \mathbf{D}_c^{-1} \mathbf{D}_1 \boldsymbol{\epsilon}_1^0 + V_2 \mathbf{D}_c^{-1} \mathbf{D}_2 \boldsymbol{\epsilon}_2^0 \tag{23}$$

where $\boldsymbol{\epsilon}_1^0$ and $\boldsymbol{\epsilon}_2^0$ are the constituents free hygroexpansion strains. A general expression for k number of material is

$$\boldsymbol{\epsilon}^0 = \sum_{i=1}^{k} V_i \mathbf{D}_c^{-1} \mathbf{D}_i \boldsymbol{\epsilon}_i^0 \tag{24}$$

and the integration for all fibres in a network is

$$\boldsymbol{\epsilon}_f^0 = \mathbf{D}_c^{-1} \int_0^\pi \boldsymbol{\sigma} \cdot f(\varphi) d\varphi = \int_0^\pi \mathbf{D}_c^{-1} \mathbf{T}^{-1} \overline{\mathbf{D}} \overline{\boldsymbol{\epsilon}}^0 \cdot f(\varphi) d\varphi \tag{25}$$

or

$$\boldsymbol{\epsilon}_f^0 = \int_0^\pi \mathbf{D}_c^{-1} \mathbf{D} \mathbf{T}^T \overline{\boldsymbol{\epsilon}}^0 \cdot f(\varphi) d\varphi \tag{26}$$

5 An interpolation model

The idea of this model is to make a mathematical interpolation between the cases of parallel and serial coupling. One way to achieve this is by inserting a potence, "α" over all matrices. The parameter α works as a fitting parameter and can be fitted to measurements but also estimated regarding to the geometry of the composite.

$$\mathbf{D}_c^\alpha = V_m \mathbf{D}_m^\alpha + V_f \mathbf{D}_f^\alpha \tag{27}$$

here $\alpha = 1$ corresponds to the parallel coupling case and $\alpha = -1$ corresponds to the serial coupling case. The idea comes from the compendium in building materials [7] where it is described in one dimension, i.e. for scalar properties:

$$E_c^\alpha = V_m E_m^\alpha + V_f E_f^\alpha \tag{28}$$

which for $n \to 0$ appproaches

$$E_c = E_m^{V_m} E_f^{V_f} \tag{29}$$

which is the geometrical mean of E_m och E_f.

According to Wall [8] even the Halpion-Tsai equations can be seen as an interpolation between arithmetic mean, $\alpha = 1$, and harmonic mean, $\alpha = -1$. He also mensions the weighted potence mean, equation (28), for scalar properties.

5.1 Calculation of $\mathbf{D}^\alpha$

The potence, α, inserted is an operation carried out on the entire matrix, and not elementwise. Like other matrix functions this operation is done by diagonalising the matrix and performing the operation on the diagonal elements

$$\mathbf{D}^\alpha = (\mathbf{Q}\mathbf{\Lambda}\mathbf{Q}^{-1})^\alpha = \mathbf{Q}(\mathbf{\Lambda})^\alpha\mathbf{Q}^{-1} = \mathbf{Q}\begin{bmatrix} \lambda_1^\alpha & 0 & 0 \\ 0 & \lambda_2^\alpha & 0 \\ 0 & 0 & \lambda_3^\alpha \end{bmatrix}\mathbf{Q}^{-1} \tag{30}$$

The requirement for this to be possible is that $\mathbf{D}$ is diagonalisable and positively difinite, which easily can be shown if $\mathbf{D}$ is linear elastic.

5.2 Problem

Now the corresponding procedure for hygroexpansion is analysed. For a composite with two constituents the equations (19) and (23) are combined to

$$\boldsymbol{\epsilon}^0 = V_1(\mathbf{D}_c^{-1}\mathbf{D}_1)^{\frac{\alpha+1}{2}}\boldsymbol{\epsilon}_1^0 + V_2(\mathbf{D}_c^{-1}\mathbf{D}_2)^{\frac{\alpha+1}{2}}\boldsymbol{\epsilon}_2^0 \tag{31}$$

Still $\alpha = 1$ corresponds to parallel coupling and $\alpha = -1$ to serial coupling. One small problem is that the strain $\boldsymbol{\epsilon}_c^0$ not equals the free strains of the constituents when they are set to be equal $\boldsymbol{\epsilon}_1^0 = \boldsymbol{\epsilon}_2^0$ for all α. $\boldsymbol{\epsilon}_c^0$ is only equal to $\boldsymbol{\epsilon}_1^0$ and $\boldsymbol{\epsilon}_2^0$ when $\alpha = 1$ or $\alpha = -1$.

It is desirable to perform the calculation of the stiffness matrix and the hygroexpansion strain for a fibre network for all α even for the integration of the fibre orienation directions.

$$\mathbf{D}_f = \left[\int_0^\pi (\mathbf{T}^{-1}\overline{\mathbf{D}}\mathbf{T}^{-T})^\alpha \cdot f(\varphi)d\varphi\right]^{1/\alpha} \tag{32}$$

and for hygroexpansion

$$\boldsymbol{\epsilon}_f^0 = \int_0^\pi (\mathbf{D}_c^{-1}\mathbf{D})^{\frac{\alpha+1}{2}}\mathbf{T}^T\overline{\boldsymbol{\epsilon}}^0 \cdot f(\varphi)d\varphi \tag{33}$$

The big problem is that this calculation of $\mathbf{D}_f$ is depending on the coordinate system used. When equation (27) is solved it is natural to chose the coordinate system in the fibres direction of orthotropy (MD), but now the fibres will be weighted differently depending on the alignment. Regardless of this fact it is unacceptable for a fysical law to be dependent on the chosen coordinate system. One example is

$$\mathbf{D}_c^\alpha = V_m \mathbf{D}_m^\alpha + V_f \mathbf{D}_f^\alpha$$

which for another arbitrary chosen coordinate system can be written as

$$(\mathbf{T}^{-1}\overline{\mathbf{D}}_c\mathbf{T}^{-T})^\alpha = V_m(\mathbf{T}^{-1}\overline{\mathbf{D}}_m\mathbf{T}^{-T})^\alpha + V_f(\mathbf{T}^{-1}\overline{\mathbf{D}}_f\mathbf{T}^{-T})^\alpha$$

In order to make this coordinate invariant there have to be a way of getting rid of all $\mathbf{T}$. For example

$$(\mathbf{T}^{-1})^\alpha\overline{\mathbf{D}}_c^\alpha(\mathbf{T}^{-T})^\alpha = V_m(\mathbf{T}^{-1})^\alpha\overline{\mathbf{D}}_f^\alpha(\mathbf{T}^{-T})^\alpha + V_f(\mathbf{T}^{-1})^\alpha\overline{\mathbf{D}}_m^\alpha(\mathbf{T}^{-T})^\alpha \qquad (34)$$

Unfortunatly this simplification, or any other, is not possible since

$$\mathbf{A}^\alpha\mathbf{B}^\alpha \neq (\mathbf{AB})^\alpha \qquad (35)$$

thus the coordinate invariance not can be shown.

5.3 Redefinition of stress and strain vectors

The solution of the problem of coordinate invariance is defining the stress and strain vectors as

$$\boldsymbol{\sigma} = \begin{bmatrix} \sigma_x \\ \sigma_y \\ \sqrt{2}\,\sigma_{xy} \end{bmatrix}, \; \boldsymbol{\epsilon} = \begin{bmatrix} \epsilon_x \\ \epsilon_y \\ \sqrt{2}\,\epsilon_{xy} \end{bmatrix} \tag{36}$$

This is not new, it is mentioned in The Mechanics of Constitutive Modelling [10] briefly together with a few references. With this definition the stress and strain vectors are transformed using the same transformation matrix,

$$\overline{\boldsymbol{\sigma}} = \mathbf{T}\boldsymbol{\sigma}, \; \overline{\boldsymbol{\epsilon}} = \mathbf{T}\boldsymbol{\epsilon}, \tag{37}$$

The, now orthogonal, transformation matrix is defined as

$$\mathbf{T} = \begin{bmatrix} m^2 & n^2 & \sqrt{2}mn \\ n^2 & m^2 & -\sqrt{2}mn \\ -\sqrt{2}mn & \sqrt{2}mn & m^2 - n^2 \end{bmatrix} \tag{38}$$

5.4 Some matrix theory

The reason of defining the shear strain and shear stress components with the factor $\sqrt{2}$ instead of as in equation(2), (4) and (5) is that the stiffness matrix, $\mathbf{D}$, now is independent of in which coordinate system it is calculated. The new choice of strain and stiffness definitions gives the two necessary properties:

1) The stiffness matrix is symmetric and positively definite. This can be shown by using thermodynamics which states that the strain energy, W, allways is positive when the strains are not equal to zero. This can be written

$$W = \frac{1}{2}\boldsymbol{\epsilon}^T \mathbf{D} \boldsymbol{\epsilon} < 0 \tag{39}$$

which is equivalent to $\mathbf{D}$ being positively definite. In that case the spectre of the matrix is positive, i.e. all eigenvalues of $\mathbf{D}$ are positive if the matrix is symmetric. This means that there are no unpleasant involvements of complex numbers which arises when a negative base is raised to non-integer potence.

2) The transformation of the strains are carried out in the same way as for the stresses. This is decisive when the coordinate invariance is shown. The

constitutive relation is now:

$$\overline{\boldsymbol{\sigma}} = \overline{\mathbf{D}}\overline{\boldsymbol{\epsilon}} = \frac{1}{1-\nu_{xy}\nu_{yx}} \begin{bmatrix} E_x & \nu_x E_y & 0 \\ \nu_x E_y & E_y & 0 \\ 0 & 0 & (1-\nu_{xy}\nu_{yx}) \cdot 2G_{xy} \end{bmatrix} \overline{\boldsymbol{\epsilon}} \qquad (40)$$

The stiffness matrix is transformed as

$$\boldsymbol{\sigma} = \mathbf{T}^{-1}\overline{\boldsymbol{\sigma}} = \mathbf{T}^{-1}\overline{\mathbf{D}}\overline{\boldsymbol{\epsilon}} = \mathbf{T}^{-1}\overline{\mathbf{D}}\mathbf{T}\boldsymbol{\epsilon}$$

$$\Rightarrow$$

$$\mathbf{D} = \mathbf{T}^{-1}\overline{\mathbf{D}}\mathbf{T} \qquad (41)$$

When the engineering strains (5) are used only condition 1) is fulfilled and when the tensor components (4) are used only condition 2) is fulfilled. With the new definition both conditions are fulfilled.

When the coordinate invariance of the stiffness matrix is to be shown, the following equation is used [11]

$$f(\mathbf{B}^{-1}\mathbf{A}\mathbf{B}) = \mathbf{B}^{-1}f(\mathbf{A})\mathbf{B} \qquad (42)$$

where f is a arbitrary function defined on As specter, which is the set of As eigenvalues. $\mathbf{B}$ is an arbitrary inversible matrix. Observe the similarity with equation (30). The equation (42) can be proved by potence serie expanding the function $f(\mathbf{B}^{-1}\mathbf{AB})$. The equation

$$\mathbf{D}_c^\alpha = V_m \mathbf{D}_m^\alpha + V_f \mathbf{D}_f^\alpha \tag{43}$$

can now in an arbitrarily oriented coordinate system be written

$$(\mathbf{T}^{-1}\overline{\mathbf{D}}_c\mathbf{T})^\alpha = V_m(\mathbf{T}^{-1}\overline{\mathbf{D}}_m\mathbf{T})^\alpha + V_f(\mathbf{T}^{-1}\overline{\mathbf{D}}_f\mathbf{T})^\alpha$$

With equation (42) this gives

$$\mathbf{T}^{-1}\overline{\mathbf{D}}_c^\alpha\mathbf{T} = V_m\mathbf{T}^{-1}\overline{\mathbf{D}}_c^\alpha\mathbf{T} + V_f\mathbf{T}^{-1}\overline{\mathbf{D}}_f^\alpha\mathbf{T}$$

Multiplication with $\mathbf{T}$ from left and with $\mathbf{T}^{-1}$ from right gives

$$\overline{\mathbf{D}}_c^\alpha = V_m\overline{\mathbf{D}}_c^\alpha + V_f\overline{\mathbf{D}}_f^\alpha \tag{44}$$

and the coordinate invariance is proved.

6 Generalisation to three dimensions

In the three dimensional case the fibre orientation is described as a projection on a unit semisphere with the radius 1. The spherical coordinates on the semisphere represent the two angles, φ and θ, where θ is the angle between the positive z-axis ($0 \leq \theta \leq \pi$) and the fibre and φ is the angle between the fibres projection at the X-Y plane and the X-axis in the positive direction ($0 \leq \varphi \leq \pi$). The angles are shown in figure 3.

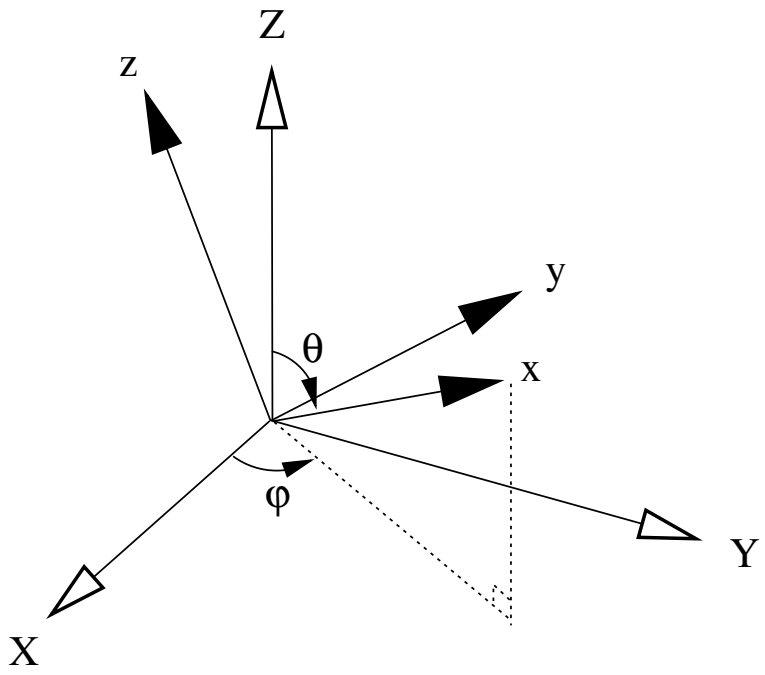

Figur 3: *Coordinate transformation in three dimensions.*

The coordinate system of the fibre has been chosen such that the x-axis coincides with the fibres longitudinal direction. The fibres are assumed to have transversaly isotropic stiffness properties in the $y-z$ plane. This means that the y-axis principally can be chosen arbitrily, orthogonal to the x-axis, but simplest is to place it in the X-Y plane, i.e.

$$\overline{\boldsymbol{e}}_y = \frac{\boldsymbol{e}_Z \times \overline{\boldsymbol{e}}_x}{|\boldsymbol{e}_Z \times \overline{\boldsymbol{e}}_x|} \tag{45}$$

6.1 Coordinate transformation

The change of base from the the local coordinate system of the fibre, (x, y, z), to the global, (X, Y, Z), is defined such that the transformation of the stress becomes

$$\overline{\boldsymbol{\sigma}} = \mathbf{T}\boldsymbol{\sigma} \tag{46}$$

where the stress in the fibres coordinates, $\overline{\boldsymbol{\sigma}}$, and in the global coordinates, $\boldsymbol{\sigma}$, are defined

$$\overline{\boldsymbol{\sigma}} = \begin{bmatrix} \sigma_x \\ \sigma_y \\ \sigma_z \\ \sqrt{2}\tau_{xy} \\ \sqrt{2}\tau_{xz} \\ \sqrt{2}\tau_{yz} \end{bmatrix}, \boldsymbol{\sigma} = \begin{bmatrix} \sigma_X \\ \sigma_Y \\ \sigma_Z \\ \sqrt{2}\tau_{XY} \\ \sqrt{2}\tau_{XZ} \\ \sqrt{2}\tau_{YZ} \end{bmatrix} \tag{47}$$

The transformation matrix, $\mathbf{T}$, is derived first by deciding the transformation of the stress and strain tensor

$$\sigma_{ij} = a_{iq} a_{jm} \overline{\sigma}_{qm} \tag{48}$$

where a_{ij} according to basic linear algebra are derived

$$[a_{ij}] = \begin{bmatrix} sm & sn & c \\ sn & m & -cn \\ c & 0 & s \end{bmatrix} \tag{49}$$

Then the components of σ_{ij} are identified at which the transformation matrix, after a correction with a factor $\sqrt{2}$, can be written

$$\mathbf{T} = \begin{bmatrix} s^2m^2 & s^2n^2 & c^2 & \sqrt{2}s^2mn & \sqrt{2}csm & \sqrt{2}csn \\ n^2 & m^2 & 0 & -\sqrt{2}mn & 0 & 0 \\ c^2m^2 & c^2n^2 & s^2 & \sqrt{2}c^2mn & -\sqrt{2}csm & -\sqrt{2}csn \\ -\sqrt{2}smn & \sqrt{2}smn & 0 & s(m^2-n^2) & -cn & cm \\ -\sqrt{2}csm^2 & -\sqrt{2}csn^2 & \sqrt{2}cs & -2csmn & -m(c^2-s^2) & -n(c^2-s^2) \\ \sqrt{2}cmn & -\sqrt{2}cmn & 0 & -c(m^2-n^2) & -sn & sm \end{bmatrix} \tag{50}$$

where the cosine and the sine of the angles are

$$\begin{aligned} m &= \cos\varphi \\ n &= \sin\varphi \\ c &= \cos\theta \\ s &= \sin\theta \end{aligned} \tag{51}$$

The strains are transformed identically

$$\overline{\boldsymbol{\epsilon}} = \mathbf{T}\boldsymbol{\epsilon} \tag{52}$$

with

$$\overline{\boldsymbol{\epsilon}} = \begin{bmatrix} \epsilon_x \\ \epsilon_y \\ \epsilon_z \\ \sqrt{2}\epsilon_{xy} \\ \sqrt{2}\epsilon_{xz} \\ \sqrt{2}\epsilon_{yz} \end{bmatrix}, \boldsymbol{\epsilon} = \begin{bmatrix} \epsilon_X \\ \epsilon_Y \\ \epsilon_Z \\ \sqrt{2}\epsilon_{XY} \\ \sqrt{2}\epsilon_{XZ} \\ \sqrt{2}\epsilon_{YZ} \end{bmatrix} \tag{53}$$

The transformation of the stiffness matrix is now like before

$$\mathbf{D} = \mathbf{T}^{-1}\overline{\mathbf{D}}\mathbf{T} \tag{54}$$

6.2 Orientation distribution function

The three dimensional distribution function, $\Psi(\varphi, \theta)$, indicates how high the fibre density is in a certain direction. The number of fibres at the surface element dS on the unit semisphere is $V = \Psi(\varphi, \theta)dS$ and the share within a certain interval of angle, $\varphi_1 \leq \varphi \leq \varphi_2$ and $\theta_1 \leq \theta \leq \theta_2$, is

$$V = \int_{\varphi_1}^{\varphi_2} \int_{\theta_1}^{\theta_2} \Psi(\varphi, \theta) dS = \int_{\varphi_1}^{\varphi_2} \int_{\theta_1}^{\theta_2} \Psi(\varphi, \theta) \sin\theta d\varphi d\theta \tag{55}$$

since $dS = r^2 \sin\theta d\varphi d\theta = \sin\theta d\varphi d\theta$. $r^2 \sin\theta$ is a scale factor ($h_\varphi = r \sin\theta$

and $h_\theta = r$). The distribution function is assumed to be separable in the φ- and the θ direction such that

$$\Psi(\varphi, \theta) = f(\varphi) \cdot g(\theta) \tag{56}$$

where $f(\varphi)$ is the same as in the two dimensional case (12). Both function are normalised according to

$$V = \int_0^\pi \int_0^\pi \Psi(\varphi, \theta) \sin\theta d\varphi d\theta = \int_0^\pi f(\varphi) d\varphi \cdot \int_0^\pi g(\theta) \sin\theta d\theta = 1 \cdot 1 \tag{57}$$

At an isotropic distribution f and g are constants. It can easily be shown that $f = \frac{1}{\pi}$ and $g = \frac{1}{2}$. The distribution functions are assumed to be of the form

$$\begin{aligned} f(\varphi) &= A + B\cos^2\varphi \\ g(\theta) &= D + E\sin^2\theta \end{aligned} \tag{58}$$

With this form it is very easy to evaluate the integral of the transformed stiffness matrices.

6.3 Integration of all fibres

Now the stiffnesses are summarised for all fibres according to the assumption of homogeneous strain

$$\mathbf{D}_f = \int_0^{\pi} \int_0^{\pi} \mathbf{T}^{-1} \overline{\mathbf{D}} \mathbf{T} \cdot \Psi(\varphi, \theta) \sin\theta \, d\varphi d\theta \tag{59}$$

It is also here possible to perform the interpolation using the parameter α

$$\mathbf{D}_f = \left[\int_0^{\pi} \int_0^{\pi} \mathbf{T}^{-1} \overline{\mathbf{D}}^{\alpha} \mathbf{T} \cdot \Psi(\varphi, \theta) \sin\theta \, d\varphi d\theta \right]^{1/\alpha} \tag{60}$$

7 Concluding remarks

This report describes how the stresses and strains are transformed in the plane as well as in the space. This have made it possible to summarise the fibres and the matrix material stiffness matrices to different kinds of means for the entire composite under the state och homogeneous strain and homogeneous state of stress. This corresponds to the upper and the lower extreme values for the stiffness of the composite. Analogous moisture induced strain, hygroexpansion, have been summarised, which also can be used e.g. at strains caused by an increase in temperature.

The novelty here is the interpolation between the cases of parallel coupling and serial coupling according to the method of weighted potence mean is expanded from usage on scalar properties to usage on material stiffness properties at two- and three dimensional states of stress. The parameter, α, controlling the interpolation can be adapted to fit measurement data or eventually be estimated according to the geometry of the composite. By a suitable definition of stress and strain vectors the interpolation method has been shown to be coordinate invariant and computed stiffnesses are thus unambigous.

One drawback using the model in its present form is that it does not take the geometry of the fibres into consideration. One example is if it would be applied on a glassfibre-epoxy composite where the fibres as well as the matrix material are isotropic and where all fibres are aligned in one direction. The longitudinal and transversal stiffensses differ often, typically with a factor 3-4, which can not be predicted by this model. One interpretation is that the material have different α in the different directions. In order to take the fibre geometries in consideration there might be a possibility of performing som sort of homogenisation of a single fibre in a small environment of matrix material.

7.1 Future work

A similair interpolation between serial and parallel coupling for hygroexpansion were studied. One problem here was that the function did not behave in a, physically speaking, reliable way in all situations. One example is when both components hygroexpansion properties where set to be equal. Then the composites hygroexpansion should be equal to the of the comsitituents. The hygroexpansion was equal to the constituents for the cases of $\alpha = 1$ and $\alpha = -1$, but not in between. One alternative, although not as elegant

mathematically speaking, is to make a linear interpolation between parallel coupling and serial coupling

$$\boldsymbol{\epsilon}_c^0 = \frac{1+\alpha}{2}\boldsymbol{\epsilon}_p^0 + \frac{1-\alpha}{2}\boldsymbol{\epsilon}_s^0 \tag{61}$$

where $\boldsymbol{\epsilon}_p^0$ is the composites free hygroexpansion computed under parallel coupling and $\boldsymbol{\epsilon}_s^0$ under serial coupling. Other possibilities can also come into consideration.

One detail worth investigation is what happens at when $\alpha \to 0$ which corresponds to the geometrical mean. It is uncertain if it is as easy as in the scalar case, equation (29), and if it is unambigous. It may not be of greater practical importance since it is possible to choose a value of α sufficiently close to 0. But it is still desirable to show that the theory is defined in the entire interval $-1 \leq \alpha \leq 1$.

Referenser

[1] Aboudi, J. Mechanics of Composite Materials, Elsevier, NY (1991)

[2] Hashin, Z. The Elastic Moduli of Fiber-Reinforced Materials, Journal of Applied Mechanics (1964)

[3] Heyden, S. A Network Model Applied to Cellulose Fibre Materials, Progress in Paper Physics (1996)

[4] Halpin, JC. Kardos, JC. The Halpin-Tsai equations: A review. Polym. Eng. Sci. (1976)

[5] Benham, PP. Mechanics of Engineering Materials, Addison, Harlow (1996)

[6] Heyden, S. How to derive an analytical network mechanics theory, Division of Structural Mechanics, Lund University (1998)

[7] Hillerborg, A. Kompendium i Byggnadsmateriallära FK, Lund (1986)

[8] Wall, P. A Comparison of Homogenisation, Hashin-Shtrikman Bounds and the Halpin-Tsai Equations, Institutionen för Matematik, Luleå Tekniska Universitet (1994)

[9] Nevander, LE. Fukthandbok. Svensk byggtjänst, Schmids (1981)

[10] Ottosen, NS. Ristinmaa, M, The Mechanics of Constitutive Modelling, Division of Solid Mechanics, Lund University (1996)

[11] Spanne, S. Föreläsningar i matristeori, Department of Mathematics, Lund University (1994)

III

A 3D Model for Analysis of Stiffness and Hygroexpansion Properties of Fibre Composite Materials

Kristian Stålne and Per Johan Gustafsson
Division of Structural Mechanics
Lund University, Sweden

A 3D Model for Analysis of Stiffness and Hygroexpansion Properties of Fibre Composite Materials

Kristian Stålne*, Per-Johan Gustafsson†

Keywords: wood, fibre, particle, composite, analytical, modelling, stiffness, hygroexpansion, homogenisation

Abstract

A three dimensional model for stiffness and hygroexpansion of fibre and particle composite materials is presented. The model is divided into two steps, first a homogenisation of a single fibre with a coating representing the matrix material, then a network mechanics modelling of the assembly of coated fibres that constitutes the composite material. The network modelling is made by a fibre orientation integration including a linear and an exponential interpolation between the extreme case of homogenous strain and the extreme case of homogenous stress. A comparison between the modelled prediction and measurement data are made for stiffness, Poissons ratio and hygroexpansion. The matrix material is assumed to have isotropic properties and the fibre or particle material may have arbitrary orthotropic properties.

*Grad. Student, Div. of Structural Mechanics, Lund University, P.O. Box 118, S-221 00 Lund, Sweden. E-mail: kristian.stalne@byggmek.lth.se

†Prof., Div. of Structural Mechanics, Lund University, P.O. Box 118, S-221 00 Lund, Sweden. E-mail: bmpjg@byggmek.lth.se

1 INTRODUCTION

The use of advanced wood fibre composite materials is increasing in building and automotive industry applications. In the building industry, the market for high pressure laminates, HPL, made up of layers of impregnated paper, has seen a strong development during the last decade. HPL is a water-resistant material, and its surface can be made very durable and be given almost any appearance of wood. A key issue for present and future usage of products made of wood fibre composites such as HPL is shape stability. Very often, moisture-induced deformations and shape instability are the limiting factors. In this study a new composite model for the analysis of hygroexpansion properties and stiffness is discussed. The aim is to develop a model by which the 3D stiffness and hygroexpansion can be predicted, making it possible to make a good and rational design of wood fibre and particle composite materials.

For analysis of the in-plane orthotropic stiffness of fibre materials such as paper, several network mechanics models have been proposed, both analytical and numerical [4], [10]. For stiffness analysis of composites made up of unidirectional fibres and a continuous matrix material, the model of Halpin and Tsai [8] is the most frequently used. Boundaries for stiffness have also been developed, e.g. the Reuss and the Voigt approximations [1] which are valid for a general composite and the Hashin-Shtrikman bounds [9] for the effective elastic moduli of unidirectional fibre composites. Theoretical analysis of the influence of fibre length and orientation distribution on stiffness have been made by Fu *et al.* [7], Sayers [14] and Dunn *et al.* [6], who have a large list of further references. It appears that modelling of hygroexpansion or the confinement stress at restricted expansion has been awarded much less interest.

The model discussed here focuses on analytical composite modelling of 3D stiffness and hygroexpansion properties, taking into account geometrical shape, anisotropic properties and arbitrary orientation distribution of the particles. The model is developed from rigorous elasticity calculations, and relates to long fibre materials such as HPL, to short fibre materials made up of short fragments of wood fibres and a polymer matrix material, and to composites made up of pieces of wood such as a particle board. It may also be applied to network materials such as paper without any matrix material. Dunn *et al.* state that no model exists that satisfies all the theoretical benchmarks that should be used to validate any model. The model discussed here possesses such qualities as symmetric resulting stiffness matrix, correct results in the high and low concentration limits, and coincidence with the exact solutions that exist for the extreme cases of laminate geometries and continuous-fibre systems with equal shear ridgities.

The constituents are assumed to be orthotropic and linear elastic and without any chemical interaction or absorption of matrix material into the fibre walls. Time and rate effects such as creep and mechanosorption are not considered. The orientation distribution of the fibres is defined by $\psi(\varphi, \theta)$, where $0 \leq \varphi \leq \pi$ denotes the in-plane angle with the global $x-$axis and $0 \leq \theta \leq \pi$ denotes the out-of-plane angle.

2 OUTLINE OF MODEL

The model is a two-step composite model with calculation of homogenized material properties at two levels of the material structure. First, a model for the properties of a single fibre or particle with a coating representing the matrix material is developed. Then a network mechanics model is developed for the composite material made up of the fibres with a coating. The homogenized material representing a single fibre or particle with a coating is, in the following, called the *cf*-material, *cf* indicating coated fibre.

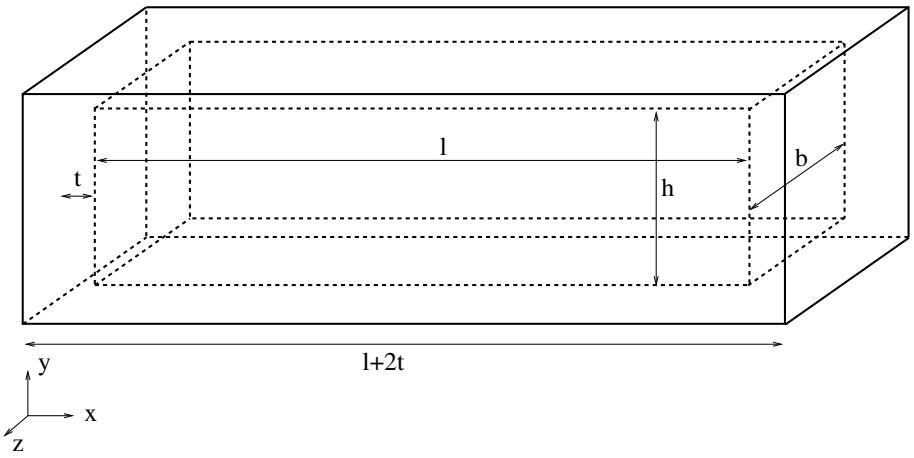

Figure 1: Fibre, $l \times b \times h$, coated with a matrix material layer with thickness t.

The fibre is assumed to have the shape of a right angle block and the coating is assumed to be of equal thickness, t, at all surfaces of the fibre, Figure 1. Knowing the shape and volume of the fibre, $V_f = lbh$, and of the matrix material, $V_m = (l + 2t)(b + 2t)(h + 2t) - lbh$, the thickness t can be calculated from the fibre to matrix volume ratio,

$$\frac{V_f}{V_m} = \frac{lbh}{(l + 2t)(b + 2t)(h + 2t) - lbh} \quad . \tag{1}$$

The total volume is $V_{tot} = V_f + V_m + V_p$, where V_p is the volume of possible pores. The fibre volume fraction is

$$v_f = \frac{V_f}{V_{tot}} \quad . \tag{2}$$

The properties of the *cf*-material are in general orthotropic due to the more or less oblong shape of the fibre and due to orthotropic properties of the fibre. The homogenised properties of the composite material are obtained by integration over the fibre orientation directions. This integration is made with respect to a function containing the properties of the *cf*-material. This function has a free parameter, $\alpha, -1 \leq \alpha \leq 1$, such that $\alpha = 1$ corresponds to the extreme of parallel coupling with complete interaction and equal strain for the variously oriented *cf*-material, and $\alpha = -1$ corresponds to the extreme of series coupling with equal stress. Two types of functions of α are studied: a linear function and an exponential function.

3 HOMOGENISATION OF COATED FIBRE

The general principle used for calculating the properties of the homogenous *cf*-material is that the response to load and to moisture change should be the same in terms of deformation of the *cf*-material and the coated fibre composite structure. In the present analysis the response of the composite structure is determined by minimization of potential energy. This minimization is carried out to a finite number of parameters, degrees of freedom, which, together with an assumption regarding the shape of the deformed structure, defines the strains. The present choice of shape functions fulfills the conditions of compatibility. Hence the calculated stiffness of the structure will, in general, somewhat overestimate the true stiffness. The deformed shape valid for loading by normal force in the $x-, y-$ or $z-$direction and for the change of moisture content is, for the 3D case, defined by 3 times 2 normal strain parameters, see Figure 2b. The shape for shear loadings is defined by 3 times 3 independent shear strain parameters, see Figure 2c.

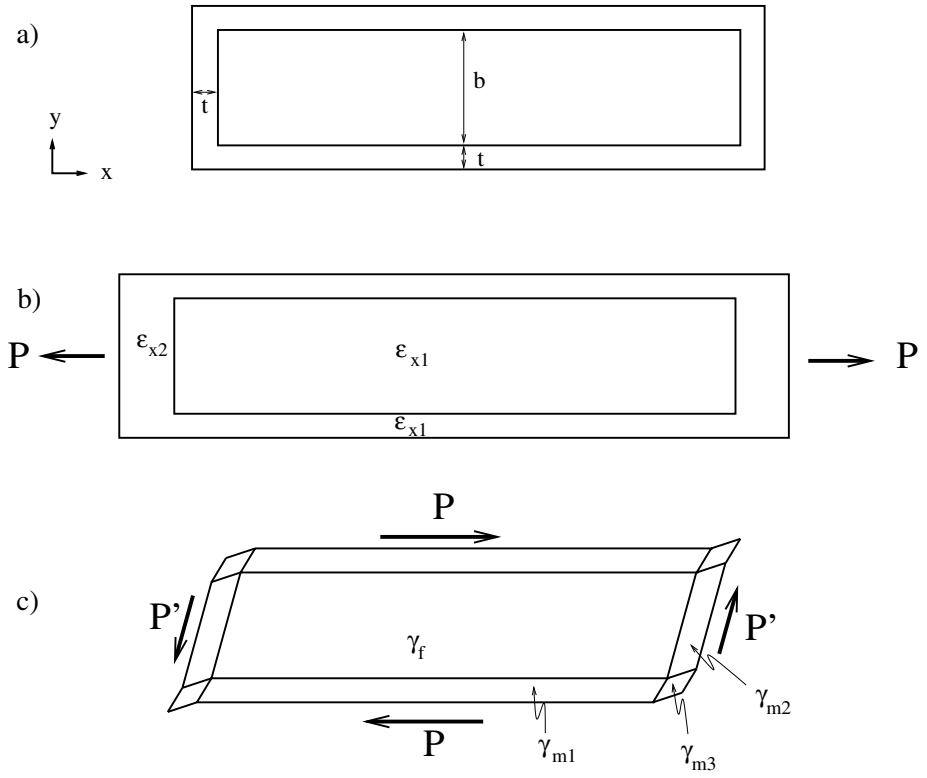

Figure 2: Shape of coated fibre, a) unloaded, b) loaded in tension, c) loaded in shear.

The potential energy for a structure or body and the loads acting on the body is

$$\Pi = U - W = \frac{1}{2}\int_V \varepsilon^T \boldsymbol{\sigma} dV - \int_S \mathbf{u}^T \mathbf{f} dS \tag{3}$$

where U is the strain energy and W is the potential energy of the loads. Minimization of Π with respect to the free parameters

$$\frac{\partial \Pi}{\partial \varepsilon'} = 0, \tag{4}$$

provides the equations from which the free strain parameters can be calculated.

3.1 E-moduli and Poissons ratios of *cf*-material

The stiffness properties of the homogenized *cf*-material are defined by a 6×6 compliance matrix, $\overline{\mathbf{C}}_{cf}$, relating a stress vector and a strain vector $\overline{\varepsilon} = \overline{\mathbf{C}}_{cf}\ \overline{\sigma}$ in the local coordinate system of the *cf*

$$\begin{bmatrix} \varepsilon_x \\ \varepsilon_y \\ \varepsilon_z \\ \sqrt{2}\varepsilon_{xy} \\ \sqrt{2}\varepsilon_{xz} \\ \sqrt{2}\varepsilon_{yz} \end{bmatrix} = \begin{bmatrix} \frac{1}{E_x} & -\frac{\nu_{yx}}{E_y} & -\frac{\nu_{zx}}{E_z} & 0 & 0 & 0 \\ -\frac{\nu_{xy}}{E_x} & \frac{1}{E_y} & -\frac{\nu_{zy}}{E_z} & 0 & 0 & 0 \\ -\frac{\nu_{xz}}{E_x} & -\frac{\nu_{yz}}{E_y} & \frac{1}{E_z} & 0 & 0 & 0 \\ 0 & 0 & 0 & \frac{1}{2G_{xy}} & 0 & 0 \\ 0 & 0 & 0 & 0 & \frac{1}{2G_{xz}} & 0 \\ 0 & 0 & 0 & 0 & 0 & \frac{1}{2G_{yz}} \end{bmatrix} \begin{bmatrix} \sigma_x \\ \sigma_y \\ \sigma_z \\ \sqrt{2}\sigma_{xy} \\ \sqrt{2}\sigma_{xz} \\ \sqrt{2}\sigma_{yz} \end{bmatrix}. \tag{5}$$

The shear components in $\overline{\boldsymbol{\varepsilon}}$ and $\overline{\boldsymbol{\sigma}}$ are defined with a factor $\sqrt{2}$ which facilitates subsequal analysis of the composite material. The six independent elastic stiffness parameters in the upper left of $\overline{\mathbf{C}}_{cf}$ are obtained by analysing the performance of the *cf* structure when exposed to normal force, Figure 2b. The three shear stiffness parameters are obtained separately by analysing the performance at shear loading, Figure 2c.

The deformation during loading according to Figure 2b is defined by six parameters:

ε_{x1} - normal strain in the $x-$direction in the interval $0 \leq x \leq l$,
ε_{x2} - normal strain in the $x-$direction in the interval $l \leq x \leq l + 2t$,
ε_{y1} - normal strain in the $y-$direction in the interval $0 \leq y \leq b$,
ε_{y2} - normal strain in the $y-$direction in the interval $b \leq y \leq b + 2t$,
ε_{z1} - normal strain in the $z-$direction in the interval $0 \leq z \leq h$,
ε_{z2} - normal strain in the $z-$direction in the interval $h \leq z \leq h + 2t$.

This yields $2^3 = 8$ subvolumes, see Figure 3, with different sets of $\varepsilon_x, \varepsilon_y$ and ε_z , e.g $\overline{\boldsymbol{\varepsilon}}_f = [\, \varepsilon_{x1} \;\; \varepsilon_{y1} \;\; \varepsilon_{z1} \;\; 0 \;\; 0 \;\; 0]$ for the first subvolume, denoted f.

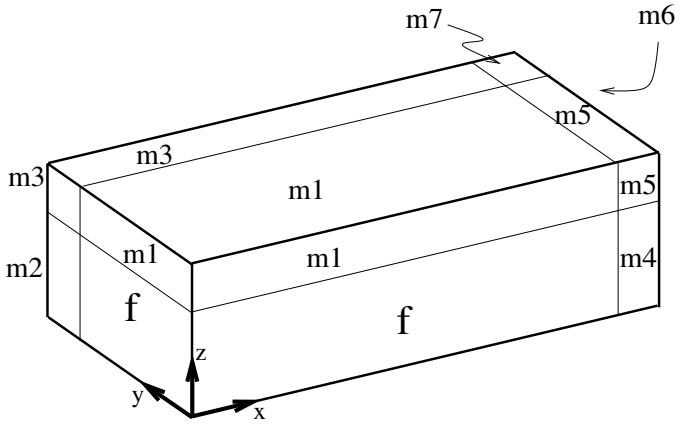

Figure 3: Subvolumes with different strain.

From equation (3)

$$\Pi = \frac{1}{2} V_f \overline{\boldsymbol{\varepsilon}}_f^T \overline{\mathbf{D}}_f \overline{\boldsymbol{\varepsilon}}_f + \sum_{i=1}^{7} \frac{1}{2} V_{mi} \overline{\boldsymbol{\varepsilon}}_{mi}^T \overline{\mathbf{D}}_m \overline{\boldsymbol{\varepsilon}}_{mi} - P(l\varepsilon_{x1} + 2t\varepsilon_{x2}) \tag{6}$$

where the stiffness matrices, $\overline{\mathbf{D}}_f$ and $\overline{\mathbf{D}}_m$ are equal to $\overline{\mathbf{C}}_f^{-1}$ and $\overline{\mathbf{C}}_m^{-1}$ defining the stiffness properties of the fibre and the matrix material respectively, in analogy with equation (5). $V_f = lbh$, $V_{m1} = 2tlb$, $V_{m2} = 2tlh, \ldots$ etc are the volumes of the respective region. Partial derivatives, equation (4), with respect to the six free parameters, $\boldsymbol{\varepsilon}' = [\varepsilon_{x1}, \varepsilon_{x2}, \varepsilon_{y1}, \varepsilon_{y2}, \varepsilon_{z1}, \varepsilon_{z2}]^T$, gives, for loading in the x-direction, a system of equations

$$\begin{cases}
V_f \mathbf{e}_x^T \overline{\mathbf{D}}_f \overline{\boldsymbol{\varepsilon}}_f + V_{m1} \mathbf{e}_x^T \overline{\mathbf{D}}_m \overline{\boldsymbol{\varepsilon}}_{m1} + V_{m2} \mathbf{e}_x^T \overline{\mathbf{D}}_m \overline{\boldsymbol{\varepsilon}}_{m2} + V_{m3} \mathbf{e}_x^T \overline{\mathbf{D}}_m \overline{\boldsymbol{\varepsilon}}_{m3} = Pl \\
V_f \mathbf{e}_y^T \overline{\mathbf{D}}_f \overline{\boldsymbol{\varepsilon}}_f + V_{m1} \mathbf{e}_y^T \overline{\mathbf{D}}_m \overline{\boldsymbol{\varepsilon}}_{m1} + V_{m4} \mathbf{e}_y^T \overline{\mathbf{D}}_m \overline{\boldsymbol{\varepsilon}}_{m4} + V_{m5} \mathbf{e}_y^T \overline{\mathbf{D}}_m \overline{\boldsymbol{\varepsilon}}_{m5} = 0 \\
V_f \mathbf{e}_z^T \overline{\mathbf{D}}_f \overline{\boldsymbol{\varepsilon}}_f + V_{m2} \mathbf{e}_z^T \overline{\mathbf{D}}_m \overline{\boldsymbol{\varepsilon}}_{m2} + V_{m4} \mathbf{e}_z^T \overline{\mathbf{D}}_m \overline{\boldsymbol{\varepsilon}}_{m4} + V_{m6} \mathbf{e}_z^T \overline{\mathbf{D}}_m \overline{\boldsymbol{\varepsilon}}_{m6} = 0 \\
V_{m4} \mathbf{e}_x^T \overline{\mathbf{D}}_m \overline{\boldsymbol{\varepsilon}}_{m4} + V_{m5} \mathbf{e}_x^T \overline{\mathbf{D}}_m \overline{\boldsymbol{\varepsilon}}_{m5} + V_{m6} \mathbf{e}_x^T \overline{\mathbf{D}}_m \overline{\boldsymbol{\varepsilon}}_{m6} + V_{m7} \mathbf{e}_x^T \overline{\mathbf{D}}_m \overline{\boldsymbol{\varepsilon}}_{m7} = 2tP \\
V_{m2} \mathbf{e}_y^T \overline{\mathbf{D}}_m \overline{\boldsymbol{\varepsilon}}_{m2} + V_{m3} \mathbf{e}_y^T \overline{\mathbf{D}}_m \overline{\boldsymbol{\varepsilon}}_{m3} + V_{m6} \mathbf{e}_y^T \overline{\mathbf{D}}_m \overline{\boldsymbol{\varepsilon}}_{m6} + V_{m7} \mathbf{e}_y^T \overline{\mathbf{D}}_m \overline{\boldsymbol{\varepsilon}}_{m7} = 0 \\
V_{m1} \mathbf{e}_z^T \overline{\mathbf{D}}_m \overline{\boldsymbol{\varepsilon}}_{m1} + V_{m3} \mathbf{e}_z^T \overline{\mathbf{D}}_m \overline{\boldsymbol{\varepsilon}}_{m3} + V_{m5} \mathbf{e}_z^T \overline{\mathbf{D}}_m \overline{\boldsymbol{\varepsilon}}_{m5} + V_{m7} \mathbf{e}_z^T \overline{\mathbf{D}}_m \overline{\boldsymbol{\varepsilon}}_{m7} = 0
\end{cases} \tag{7}$$

where $\mathbf{e}_x^T = [1\ 0\ 0\ 0\ 0\ 0], \mathbf{e}_y^T = [0\ 1\ 0\ 0\ 0\ 0]$ and $\mathbf{e}_z^T = [0\ 0\ 1\ 0\ 0\ 0]$ are unit vectors. In matrix form this linear system of equations can be written as $\mathbf{K}_n \boldsymbol{\varepsilon}' = \mathbf{f}_x$ where $\mathbf{f}_x = P\,[l\ 0\ 0\ 2t\ 0\ 0]^T$ and $\mathbf{K}_n$ contains components from $\overline{\mathbf{D}}_f$, $\overline{\mathbf{D}}_m$ and volumes of the respective regions. When the strains have been solved, Young's modulus E_x and Poisson's ratios ν_{xy} and ν_{xz} of the *cf*-material are calculated from

$$E_x = \sigma_{x,mean} \big/ \varepsilon_{x,mean} = \frac{P}{(b+2t)(h+2t)} \Big/ \frac{l\,\varepsilon_{x1} + 2t\,\varepsilon_{x2}}{l+2t} \tag{8}$$

$$\nu_{xy} = -\frac{\varepsilon_{y,mean}}{\varepsilon_{x,mean}}, \quad \nu_{xz} = -\frac{\varepsilon_{z,mean}}{\varepsilon_{x,mean}}\ . \tag{9}$$

Properties in the other two directions are calculated analogously by redefining the force vector to $\mathbf{f}_y$ and $\mathbf{f}_z$ respectively.

3.2 Shear moduli of *cf*

The shear stiffness parameters of the *cf*-material are obtained in a similar way. Since the $x-y$-shear strain is constant in the z-direction, the assumed deformation pattern at loading in the $x-y$ plane is defined by three independent parameters, γ_f, γ_{m1} and γ_{m2}, see Figure 2c. The fourth shear strain parameter, γ_{m3}, is determined by the condition of compatibility, giving

$$\gamma_{m3} = \gamma_{m1} + \gamma_{m2} - \gamma_f\ . \tag{10}$$

From equation(3) the potential, Π, is

$$\begin{aligned}\Pi &= \frac{1}{2}V_f G_{fm}\gamma_f^2 + \frac{1}{2}V_{m1}G_m\gamma_{m1}^2 + \frac{1}{2}V_{m2}G_m\gamma_{m2}^2 + \frac{1}{2}V_{m3}G_m(\gamma_{m1}+\gamma_{m2}-\gamma_f)^2 - \\ &\quad P[(b - \frac{b+2t}{l+2t}2t)\gamma_f + 2t\gamma_{m2} + \frac{b+2t}{l+2t}2t\gamma_{m1}] \end{aligned} \tag{11}$$

where G_{fm} is the mean shear modulus of the fibre in region f and the matrix in region $m1$. In these two regions the shear strain is the same at loading in the $x-y$ plane.

$$G_{fm} = \frac{hG_f + 2tG_m}{h+2t} \tag{12}$$

where G_f and G_m are the $x-y$-plane shear moduli of the fibre and matrix, respectively. Minimization of the energy

$$\frac{\partial \Pi}{\partial \boldsymbol{\gamma}'} = 0 \tag{13}$$

where $\boldsymbol{\gamma}' = [\gamma_f \;\; \gamma_{m1} \;\; \gamma_{m2}]$ yields the shear strain parameters by solving the equation

$$\begin{bmatrix} blG_{fm} + 4t^2G_m & -4t^2G_m & -4t^2G_m \\ -4t^2G_m & (2bt+4t^2)G_m & 4t^2G_m \\ -4t^2G_m & 4t^2G_m & (2lt+4t^2)G_m \end{bmatrix} \begin{bmatrix} \gamma_f \\ \gamma_{m1} \\ \gamma_{m2} \end{bmatrix} = P \begin{bmatrix} b - 2t\frac{b+2t}{l+2t} \\ 2t \\ 2t\frac{b+2t}{l+2t} \end{bmatrix}. \tag{14}$$

Now the shear strain of the homogenised *cf*-material can be obtained from the displacements of the corners of the *cf*-structure, Figure 2c, expressed in γ_f, γ_{m1} and γ_{m2}. The shear stress in the *cf*-material when loaded by P and P' is $P/((l+2t)(h+2t)) = P'/((b+2t)(h+2t))$, giving

$$G_{xy} = \frac{\tau_{(cf)xy}}{\gamma_{(cf)xy}} = \frac{P}{(l+2t)(h+2t)} \Big/ \left(\frac{2t\gamma_{m1} + b\gamma_f}{2t+b} + \frac{2t(\gamma_{2m} - \gamma_f)}{2t+l} \right) \tag{15}$$

where G_{xy} is the shear modulus of the *cf*-material. G_{xz} and G_{yz} are calculated analogously by applying the load in the $x-z$ and $y-z$ planes respectively.

3.3 Hygroexpansion of *cf*-material

The free expansion of the fibre material is assumed to be

$$\overline{\boldsymbol{\varepsilon}}_f^o = \left[\varepsilon_{(f)x}^o \;\; \varepsilon_{(f)y}^o \;\; \varepsilon_{(f)z}^o \;\; 0 \;\; 0 \;\; 0 \right]^T \tag{16}$$

and the free hygroexpansion of the matrix material is assumed to be

$$\overline{\boldsymbol{\varepsilon}}^o_m = \left[\varepsilon^o_{(m)x} \;\; \varepsilon^o_{(m)y} \;\; \varepsilon^o_{(m)z} \;\; 0 \;\; 0 \;\; 0\right]^T \quad . \tag{17}$$

The free hygroexpansion of the constituents is thus assumed to be isotropic or orthotropic with material axes according to the axes of the fibre geometry. At free hygroexpansion of a coated fibre, any difference between $\overline{\boldsymbol{\varepsilon}}^o_f$ and $\overline{\boldsymbol{\varepsilon}}^o_m$ will in general produce stresses and normal strains in the 8 regions of the *cf*-structure. From equation (3) the potential of the structure is then

$$\Pi = \frac{1}{2} V_f (\overline{\boldsymbol{\varepsilon}}_f - \overline{\boldsymbol{\varepsilon}}^o_f)^T \overline{\mathbf{D}}_f (\overline{\boldsymbol{\varepsilon}}_f - \overline{\boldsymbol{\varepsilon}}^o_f) + \sum_{i=1}^{7} \frac{1}{2} V_{mi} (\overline{\boldsymbol{\varepsilon}}_{mi} - \overline{\boldsymbol{\varepsilon}}^o_m)^T \overline{\mathbf{D}}_m (\overline{\boldsymbol{\varepsilon}}_{mi} - \overline{\boldsymbol{\varepsilon}}^o_m) \tag{18}$$

which by minimization according to equation (4) with respect to the free parameters, $\boldsymbol{\varepsilon}' = [\varepsilon_{x1} \;\; \varepsilon_{x2} \;\; \varepsilon_{y1} \;\; \varepsilon_{y2} \;\; \varepsilon_{z1} \;\; \varepsilon_{z2}]^T$, gives a system of equations

$$\mathbf{K}_n \boldsymbol{\varepsilon}' = \mathbf{f}_{hyg} \tag{19}$$

where $\mathbf{f}_{hyg}$ contains the free hygroexpansion components from $\overline{\boldsymbol{\varepsilon}}^o_f$ and $\overline{\boldsymbol{\varepsilon}}^o_m$, and $\mathbf{K}_n$ is defined in the above, see equation (7). From this the strain parameters, $\boldsymbol{\varepsilon}'$, are solved. The free hygroexpansion of the *cf*-material in the x-, y- and the z-directions can then be calculated by summation of the strains in the different regions of the *cf*-strucutre:

$$\varepsilon_{x(cf)} = \frac{l\varepsilon_{x1} + 2t\varepsilon_{x2}}{l + 2t}, \quad \varepsilon_{y(cf)} = \frac{b\varepsilon_{y1} + 2t\varepsilon_{y2}}{b + 2t}, \quad \varepsilon_{z(cf)} = \frac{h\varepsilon_{z1} + 2t\varepsilon_{z2}}{h + 2t} \quad . \tag{20}$$

which gives the free hygroexpansion, $\overline{\boldsymbol{\varepsilon}}^o_{cf}$, of the *cf*-material. There will be no shear strain at hygroexpansion due to the assumption of orthotropic properties of the constituents.

4 HOMOGENISATION OF COATED FIBRE NETWORK

4.1 Composite material stiffness properties

The composite material is built up of coated fibres with arbitrary orientation distribution. The global coordinate system and material properties in that system are here given without overline, i.e. x, y, z, while the local coordinate system of the fibre is indicated here by an overline, $\overline{x}, \overline{y}, \overline{z}$, see Figure 4 where the $\overline{x}$-direction is the orientation of the fibre.

From the properties calculated in the previous section, a constitutive relation of the coated fibre is defined in (5), or in a shorter matrix notation

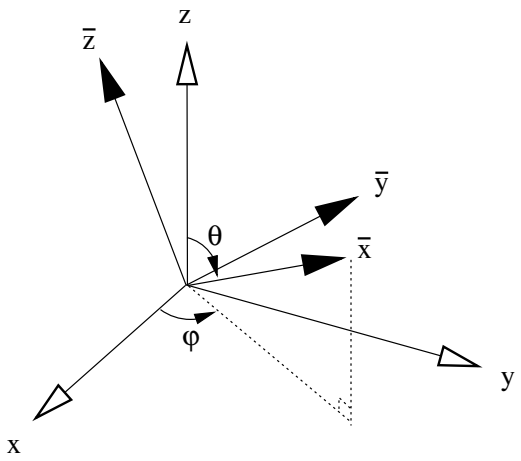

Figure 4: Three dimensional coordinate transformation. The fibre is oriented in the x-direction.

$$\overline{\boldsymbol{\varepsilon}} = \overline{\mathbf{D}}_{cf}^{-1}\overline{\boldsymbol{\sigma}} \tag{21}$$

The shear components in $\overline{\boldsymbol{\varepsilon}}$ and $\overline{\boldsymbol{\sigma}}$ are defined with a factor $\sqrt{2}$ in order to make the coordinate transformations from the local to the global coordinate system for stresses and strains identical [15], i.e.

$$\overline{\boldsymbol{\varepsilon}} = \mathbf{T}\boldsymbol{\varepsilon}, \quad \overline{\boldsymbol{\sigma}} = \mathbf{T}\boldsymbol{\sigma} \tag{22}$$

where the transformation matrix, $\mathbf{T}$, consists of sines and cosines of the rotation angles φ and θ. This is necessary to make the interpolation in (28) coordinate frame independent.

The transformation of the stiffness matrix becomes

$$\mathbf{D}_{cf} = \mathbf{T}^{-1}\overline{\mathbf{D}}_{cf}\mathbf{T} \tag{23}$$

The orientation distribution of the fibres is described with the scalar function $\psi(\varphi, \theta)$ so that the share of fibres in a small interval, $d\varphi d\theta$, is $\psi(\varphi, \theta)\sin\theta d\varphi d\theta$. ψ is in the subsequent applications assumed to have the form

$$\psi(\varphi, \theta) = f(\varphi)g(\theta) = (k_1 + k_2\cos^2\varphi)(k_3 + k_4\sin^2\theta) \tag{24}$$

where $k_1..k_4$ are distribution shape parameters. A 2-dimensional orientation distribution is achieved with $g(\theta) = \delta(\pi/2)$, the Dirac delta function.

For the homogenous strain assumption (the Voigt approximation or parallel coupling) the composite material stiffness matrix, $\mathbf{D}_{c(p)}$, is calculated by integration of the stiffness in all directions

$$\begin{aligned}\mathbf{D}_{c(p)} &= \int_0^\pi \int_0^\pi \mathbf{D}_{cf}\,\psi(\varphi,\theta)\sin\theta\,d\varphi d\theta \\ &= \int_0^\pi \int_0^\pi \mathbf{T}^{-1}\overline{\mathbf{D}}_{cf}\mathbf{T}\psi(\varphi,\theta)\sin\theta\,d\varphi d\theta\end{aligned} \tag{25}$$

For the homogenous stress assumption (the Reuss approximation or serial coupling) the stiffness matrix is calculated as the inverse of the integrated compliance according to

$$\mathbf{D}_{c(s)} = \left[\int_0^\pi \int_0^\pi \mathbf{T}^{-1}\overline{\mathbf{D}}_{cf}^{-1}\mathbf{T}\psi(\varphi,\theta)\sin\theta\,d\varphi d\theta\right]^{-1} \tag{26}$$

According to Hill's theorem these two cases are the extreme cases of the composite stiffness. A linear interpolation between the two cases gives

$$\mathbf{D}_c = \frac{1+\alpha}{2}\mathbf{D}_{c(p)} + \frac{1-\alpha}{2}\mathbf{D}_{c(s)} \tag{27}$$

where α can be considered as a fitting parameter between the Voigt approximation ($\alpha = 1$) and the Reuss approximation ($\alpha = -1$).

Another way of interpolating the Voigt and the Reuss approximations is by raising the stiffness matrices by the scalar α:

$$\mathbf{D}_{c(s)} = \left[\int_0^\pi \int_0^\pi \mathbf{T}^{-1}\overline{\mathbf{D}}_{cf}^{\alpha}\mathbf{T}\psi(\varphi,\theta)\sin\theta\,d\varphi d\theta\right]^{1/\alpha} \tag{28}$$

where, as with the linear interpolation, $\alpha = 1$ corresponds to the Voigt and $\alpha = -1$ to the Reuss. Since $\mathbf{D}_{cf}$ is positive definite in all coordinate systems, α can assume any value in between in analogy to the linear interpolation. It can by use of matrix theory be shown, see Stålne [15], that material property analysis according to equation (28) fulfills the condition of coordinate frame independence.

4.2 Composite hygroexpansion

The hygroexpansion of the coated fibre network homogenisation is first calculated by the homogenous strain assumption

$$\overline{\boldsymbol{\varepsilon}}_{c(p)} = \int_0^\pi \int_0^\pi \mathbf{D}_{c(p)}^{-1}\,\mathbf{T}^{-1}\overline{\mathbf{D}}_{cf}\overline{\boldsymbol{\varepsilon}}_{cf}^{o}\,\psi(\varphi,\theta)\sin\theta\,d\varphi d\theta \tag{29}$$

which gives the lower boundary of the free composite hygroexpansion strain. The upper boundary is given by the homogenous stress assumption

$$\overline{\varepsilon}_{c(s)} = \int_0^{\pi} \int_0^{\pi} \mathbf{T}^{-1} \overline{\varepsilon}^{o}_{cf} \psi(\varphi, \theta) \sin\theta \, d\varphi d\theta \quad . \tag{30}$$

The linear interpolation can be applied here by defining the composite hygroexpansion

$$\overline{\varepsilon}_c = \frac{1+\alpha}{2} \overline{\varepsilon}_{c(p)} + \frac{1-\alpha}{2} \overline{\varepsilon}_{c(s)} \tag{31}$$

where, as before, $\alpha = 1$ corresponds to the case of homogenous strain and $\alpha = -1$ to homogenous stress. The only plausible interpolation is this linear interpolation since the power interpolation does not give the same hygroexpansion as the constituents when all constituents hygroexpansion are set equal.

5 COMPARISON TO EXPERIMENTAL RESULTS

Results from the model are compared to results from measurements made on composites with different fibre-matrix fractions. First, the results from a study of the stiffness of a polypropylene and wood flour composite [12] are investigated. Stiffness and hygroexpansion properties are then studied in relation to an experimental study of high pressure laminates made of paper impregnated with phenolic or melamine formaldehyde resin [2].

5.1 Polypropylene-wood flour composite

Polypropylene is a synthetic polymer used in injection molded products, and it can be modified with sawdust in order to increase its stiffness. The matrix material, the polypropylene, is considered isotropic and the sawdust as particles of solid wood, pine. The fibre orientation distribution was recorded experimentally (Nilsson, L.-O.,et.al."Wood composites based on recycled plastics - mechanical properties." unpublished internal report. of Structural Mechanics, Lund University, Sweden) and the orthotropic distribution found was used in the calculation. The shape of the wood particles was determined by optical inspection to $[\ l \quad b \quad h\ ] = [\ 3 \quad 1 \quad 1\ ]$ and the interpolation parameter α was set equal to 0, being a reasonable first value in between the limits -1 and 1. This value can, if needed, be adjusted by fitting to experimental data. The mechanical properties of the wood flour listed in Table 1 are from [5] and the properties of the matrix material are determined from the tests with $v_f = 0$.

The experimental and theoretical results on composite material stiffness at various fibre volume fraction are shown in Figure 5 and in Table 2. The two

Table 1: Mechanical properties of wood flour and polypropylene.

Wood Particle									Matrix	
E_x [MPa]	E_y [MPa]	E_z [MPa]	ν_{xy} [-]	ν_{xz} [-]	ν_{yz} [-]	G_{xy} [MPa]	G_{xz} [MPa]	G_{yz} [MPa]	E [MPa]	ν [-]
16 000	1 100	570	0.42	0.51	0.68	1170	676	66	1 370	0.41

experimental values represent two composites containing polypropylenes with different melt flow index. This seems not to affect the stiffness, and is therefore not considered in the model.

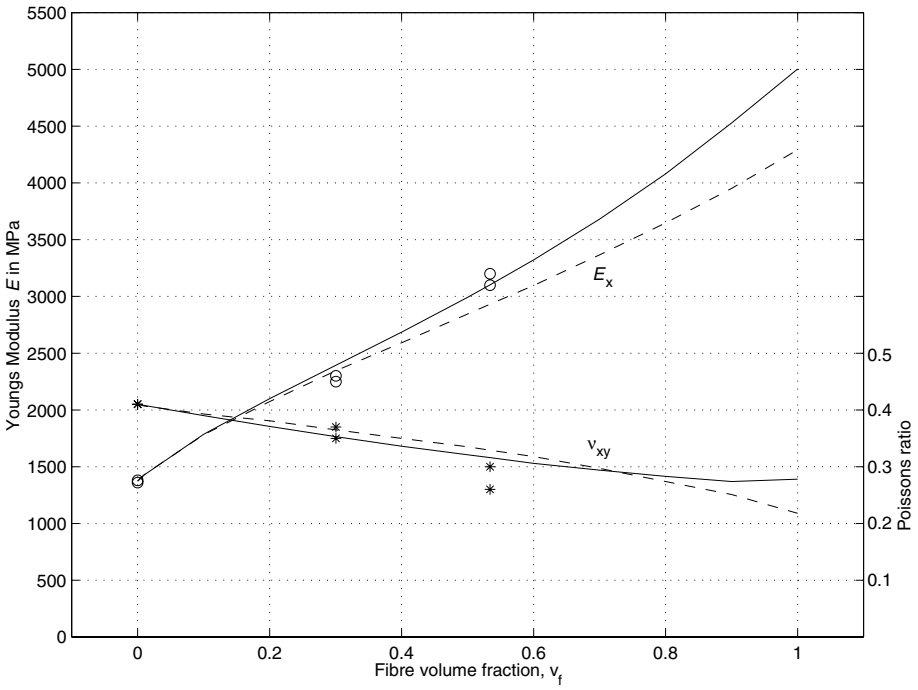

Figure 5: Experimental values of material stiffness E_x, marked with circles, and Poissons ratio ν_{xy}, marked with stars, compared with analytical modelling with linear interpolation, marked with solid lines, and with power interpolation, marked with dashed lines.

The theoretical predictions are in good agreement with the experimental results, both with respect to Youngs modulus and with respect to Poissons ratio.

Table 2: Results of measurements and modelling of polypropylene-wood flour composite.

	Measurement				Model	
	1		2			
v_f	E_X	ν	E_X	ν	E_X	ν
[-]	[MPa]	[-]	[MPa]	[-]	[MPa]	[-]
0	1380	0.41	1360	0.41	1370	0.41
0.3	2250	0.37	2300	0.35	2390	0.35
0.53	3200	0.30	3100	0.26	3100	0.31

5.2 High Pressure Laminate

A high pressure laminate (HPL) with orthotropic fibre orientation was tested for stiffness and hygroexpansion. HPL is built up of a core containing layers of phenolic resin-impregnated paper. The HPL testing was performed for tensile loading in three directions [2], and resulted in mean values of the four independent in-plane stiffness properties of an orthotropic material: 2 Youngs moduli, shear moduli and Poisons ratio, Table 4. The hygroexpansion in the two in-plane directions was measured for different intervals of the moisture content.

When modelling the HPL it is regarded as a composite with an in-plane directional orientation of continuous fibres, reflecting that the fibres are very long, $\sim$1 mm, in comparison to their width, $\sim 50\mu$m. The fibre volume fraction is measured during manufacturing to 75 per cent, and the fibre orientation distribution is considered to be 2:1 i.e. with the distribution function $f(\varphi)$ in equation (24) where the number of fibres in the x-direction is twice the number in the y-direction: $\psi(\varphi,\theta) = \frac{2}{3}\frac{1+\cos^2\varphi}{\pi} \cdot \delta(\theta{=}\pi/2)$. Exact stiffness properties for cellulose fibres are hard to estimate, e.g. an undamaged wood fibre is considered to have a longitudinal Youngs modulus of 50-60 GPa [13], which will decrease when subjected to mechanical and chemical treatment. A fibre is here assumed to have a longitudinal Youngs modulus of 40 GPa and a transversal Youngs modulus of 5 GPa, Table 3. The Youngs modulus of phenolic resin is taken from [3]. The hygroexpansion coefficient β is defined as the increase in strain per increase in moisture content in percent. Estimations of the cellulose fibre and phenolic resin hygroexpansion coefficients are from [13].

The experimental and theoretical results are summarized in Tables 4 and 5. The composite model, here used with the linear interpolation with $\alpha = 0$, appears to produce stiffness parameter values in good agreement with the experimental results. MD indicates the machine direction of the paper of the HPL, and CD

Table 3: Mechanical properties of wood fibres and phenolic resin.

Fibre						Matrix		
E_x	E_y	ν_{xy}	G_{xy}	β_x	β_y	E	ν	β
[MPa]	[MPa]	[-]	[MPa]	[1/%]	[1/%]	[MPa]	[-]	[1/%]
40 000	5 000	0.2	4 000	0.01	0.26	5 750	0.3	0.01

the cross machine direction.

Table 4: Experimental and theoretical stiffness properties of HPL.

Experimental				Theoretical			
E_{MD}	E_{CD}	G	ν	E_{MD}	E_{CD}	G	ν
[GPa]	[GPa]	[GPa]	[-]	[GPa]	[GPa]	[GPa]	[-]
15.5	10.5	4.5	0.38	14.4	10.6	3.5	0.26

Table 5: Experimental and theoretical hygroexpansion coefficients.

Experimental		Theoretical	
β_{MD}	β_{CD}	β_{MD}	β_{CD}
[1/%]	[1/%]	[1/%]	[1/%]
0.063	0.109	0.062	0.090

The hygroexpansion was measured in the interval of 35 - 65 per cent relative humidity, which corresponds to 3.5 - 5 per cent moisture content, where the expansion can be regarded as linear with increasing moisture content. In other intervals, especially at high moisture contents, the expansion is non-linear. The fairly small deviation between theoretical prediction and experimental results with respect to hygroexpansion can very well be explained by uncertainties in the material data of the composite material constituents.

6 SUMMARY AND CONCLUDING REMARKS

A three dimensional model for all stiffness and hygroexpansion components of a fibre or particle composite material has been presented. The model is divided in two steps, first a homogenisation of a simple fibre-matrix block structure and then a homogenisation of the composite material structure by an integration for

all fibre directions. The homogenisation of the coated fibre is obtained by applying normal and shear forces one by one in various directions and computing the strains by a minimization of the potential energy. Normal stiffnesses, Poissons ratios and shear stiffnesses are then determined from definition. Thereby the whole stiffness matrix can be expressed in terms of the properties of the constituents and the shape of fibre or particle.

The composite material stiffness is first obtained for the two extremes of homogenous strain and homogenous stress. This is done by integration of the stiffness or compliance matrix of the coated fibre material for all fibre directions. Analysis of the hygroexpansion properties of a coated fibre and the composite material was carried out consistent with the stiffness analysis.

Interpolation between the two extreme cases of homogenous strain and homogenous stress can be done by a simple linear weighting of the stiffness matrices or by an exponential weighting. Both interpolations have the quality of coordinate invariance. When comparing the different procedures, the exponetial approach is more appealing from a mathematial point of view, since it is unambiguous. However, the linear interpolation is simpler, more numerically stable and demands fewer calculations. When calculating the hygroexpansion the linear interpolation is the only way possible. The two interpolations appear to give fairly similar results.

The resulting stiffness matrix for the composite material is symmetric, valid in the entire range between 0 per cent and 100 per cent fibre content, and coincident with the exact solutions that exist for the extreme cases of laminate geometries and continuous-fibre systems with equal shear rigidities. At this stage, only time-independent properties of the constituents are considered in the model. Consideration of varying fibre lengths according a fibre length distribution would be easy to implement. The present model comprise some rather extensive equations. Such qualities can however be dealt with in a convenient manner by use of *MAPLE* [11] or any other similair computer code.

Comparisons between the model and measurements gave a good agreement in stiffnesses and Poissons ratio. When comparing with the measured hygroexpansion coefficients, the calculated hygroexpansion coefficients are slightly lower. The comparison to experimental results were here made only for two types of material and it can not be generally concluded that the theoretical model underestimates hygroexpansion. The model presented is flexible in such manner that it can be used in a number of different applications and contribute to a better understanding of composite material behaviour.

7 ACKNOWLEDGEMENT

This work was financed by the Swedish Wood Technology Research Colleague.

APPENDIX I.

References

[1] Aboudi, J. (1991). "Mechanics of Composite Materials", Elsevier, Amsterdam, The Netherlands, 14-18.

[2] Andersson, B. (1999). "Composite materials' hygro-mechanical properties", Masters thesis, Report TVSM-3018, Div. of Structural Mechanics, Lund University, Sweden.

[3] Barth, Th. (1984). "Der Einfluss der Feuchteaufnahme auf die mechanischen Eigenschaften von Phenolplasten." *Z. Werkstofftech*, Verlag Chemie, Weinheim, Germany, 15, 299-308.

[4] Cox, H. L. (1951). "The elasticity and strength of paper and other fibrous materials." *Brittish J. Appl. Phys.*, London, 3, 72-79.

[5] Dinwoodie, J. M. (1989). *Wood: nature's cellular, polymeric fibre-composite*, The Institute of Metals, London, 57.

[6] Dunn, M. L., Ledbetter, H., Heyliger, P. R. and Choi, C. S. (1996). "Elastic constants of textured short-fiber composites." *J. Mech. Phys. Solids*, Elsevier, Amsterdam, The Netherlands, 44, 1509-1541.

[7] Fu, S.-Y. Lauke, B. (1998). "An analytical characterization of the anisotropy of the elastic modulus of misaligned short-fiber-reinforced polymers." *Composites Sci. Techn.*, Elsevier, Amsterdam, The Netherlands, 58, 1961-1972.

[8] Halpin, J. C., Kardos, J. L. (1976). "The Halpin-Tsai equations: A review." *Polym. Eng. Sci.*, Swets, 16, 344-352.

[9] Hashin, Z., Shtrikman, S. (1963). "A variational approach to the theory of the elastic behaviour of multiphased materials." *J. Mech. Phys. Solids*, Elsevier, Amsterdam, The Netherlands, 11, 127-140.

[10] Heyden, S. (2000). *Network modelling for the evaluation of mechanical properties of cellulose fibre fluff.*, Doctoral thesis, Report TVSM-1011, Div. of Structural Mechanics, Lund University, Sweden.

[11] *MAPLE* (2000), "A symbolic computation system or computer algebra system", Version 6.0, Waterloo Maple, Inc.

[12] Nilsson, L.-O., Hjort, S., Petterson, H., Gustafsson, P. J., Molin, N.-E., Sjödahl, M., Ståhle, P., Gunnars, J., Ericson, M., Oksman, K., Vilander, Y. and Lindberg, H. (1997). "Wood composites based on recycled plastics - mechanical properties." Div. of Structural Mechanics, Lund University, Sweden.

[13] Persson, K. (1997). *Modelling of wood properties by a micromechanical approach.*, Licentiate thesis, Report TVSM-3018, Div. of Structural Mechanics, Lund University, Sweden.

[14] Sayers, C.M. (1992). "Elastic anisotropy of short-fibre reinforced composites." *Int. J. Solid Structures*, 29, 2933-2944.

[15] Stålne, K. (1999). *Analysis of fibre composite materials for stiffness and hygroexpansion*, Report TVSM-7127, Div. of Structural Mechanics, Lund University, Sweden.

APPENDIX II.

Notation

b	width of fibre
$\mathbf{C}$	compliance matrix
c	transformation angle $\cos\theta$
$\mathbf{D}$	stiffness matrix
E	Youngs moduli
$\mathbf{e}$	unit vector
$\mathbf{f}$	force vectors
$\mathbf{f}_{hyg}$	vector containing the free hygroexpansion components
f	in-x-y-plane fibre orientation distribution function
G	shear modulus
G_{fm}	mean value of shear modulus in area f
g	out-of-x-y-plane fibre orientation distribution function
h	height of fibre
$\mathbf{K}_n$	matrix containing components from $\mathbf{D}_f$ and $\mathbf{D}_m$
$\mathbf{K}_s$	matrix containing combinations of G_f and G_m
k	coefficients of the fibre orientation distribution function
l	length of fibre
m	transformation angle $\cos\varphi$
n	transformation angle $\sin\varphi$
P	tensile and shearing load on cf
s	transformation angle $\sin\theta$

$\mathbf{T}$	coordinate transformation matrix
t	thickness of matrix material coating
U	strain energy of *cf*
$\mathbf{u}$	displacement vector
V_i	volume of phase i in *cf*
v_i	volume fraction of phase i
W	potential energy of loads acting on *cf*
α	interpolation parameter
β	hygroexpansion coefficient
γ_i	shear strain in region i
δ	Dirac delta function
$\boldsymbol{\varepsilon}^o$	free hygroexpansion vector
$\boldsymbol{\varepsilon}$	strain vector
ε_{mean}	mean strain in *cf*
$\boldsymbol{\varepsilon}'$	free strain parameter vector
θ	fibre angle to the x-y-plane
ν	Poissons ratio
Π	potential energy of *cf*
$\boldsymbol{\sigma}$	stress vector
σ_{mean}	mean stress in *cf*
τ	mean shear stress in *cf*
φ	fibre in-plane angle with the x-axis
ψ	3D fibre orientation distribution function

Superscripts

-	property in local coordinate system
o	free hygroexpansion
’	free strain parameter

Subscripts

c	composite property
$c(p)$	composite property calculated in the case of homogeous strain
$c(s)$	composite property calculated in the case of homogeous stress
cf	coated fibre property
f	fibre property
m	matrix material property
mi	matrix region i
MD	paper machine direction
CD	cross paper machine direction

IV

A 3D Finite Element Fibre Network Model for Composite Material Stiffness and Hygroexpansion Analysis

Kristian Stålne and Per Johan Gustafsson
Division of Structural Mechanics
Lund University, Sweden

A 3D Finite Element Fibre Network Model for Composite Material Stiffness and Hygroexpansion Analysis

Kristian Stålne and Per Johan Gustafsson

Abstract

A 3D finite element fibre network model was developed to be used as a tool for predicting the stiffness and the hygroexpansion properties of fibre composite materials, such as high pressure laminates. The wood fibres are modelled as orthotropic or transversely isotropic solid elements surrounded by an isotropic matrix material. The fibres and the matrix are arranged in a unit cell subjected to loading or changes in moisture content. The constitutive parameters of the homogenised composite material are obtained by simulating the response of the composite structure to load and moisture. The model is evaluated by comparing the results it provides with various experimental results and with results of a recent analytical model and of various parameter studies. The model also provides in addition to properties of the homogenised material considerable information concerning stresses and strains within the material structure.

1 Introduction

High pressure laminate, HPL, is a wood fibre composite whose usage has increased much during the recent decades. It is composed of craft paper impregnated by phenolic or melamine resin. A key issue concerning wood composites is that of shape stability in relation to a moisture content gradient or to a change in moisture content. This entails the need for methods enabling the hygroexpansion and stiffness properties of wood composites such as HPL to be analysed and predicted.

Several analytical models for the stiffness of composite materials have been developed in recent decades [11, 22]. Many of these are based on the homogenisation of a single fibre surrounded by matrix material [1, 9]. These models assumes there to be no interaction between the fibres. Such an assumption is questionable in connection with HPL, however, since the particle phase of this composite material is paper, which is a network of long fibres bonded to each other.

Developments in the area of numerical simulation as based on the finite element method, for example, have made it possible to model more complicated fibre composite material structures, consisting of more than one fibre [7, 4, 6, 10, 24]. Most of these studies have dealt with estimation of the stiffness properties of plane fabric composites. These materials have a weaved fibre phase in which the fibres are crossed over and under each other at right angles [20, 8, 23, 13]. Since the fabric geometry is regular, homogenisation of a single fibre crossing is sufficient to provide a satisfactory estimate of the composite material stiffness. Composites with fibre networks of a more random types of have also been studied, using numerical simulations [15, 17, 19, 21]. There has been no study at a micro mechanical level, however, of the behaviour of composite materials of irregular geometry. Little appears to have been done either regarding simulation of the hygroexpansion or thermal expansion properties of such materials.

The aim of the model discussed is to simulate the mechanical behaviour of a wood fibre composite with an irregular fibre network, such that of paper. The model is a finite element 3D model using a square unit cell in which there are a number of fibres modelled as orthotropic solid elements surrounded by an isotropic matrix material. The response of the unit cell when exposed to an increase in moisture content and to loading in the x-, y- and z-direction, respectively, is simulated. The parameters of the model are the mechanical properties of the constituents, the fibre geometry, the fibre orientation distribution and the fibre volume fractions. The geometry of the fibres is created in a preprocessor allowing the user to decide on the location of each fibre. This enables a good rep-

resentation of the micro-structure of the fibre composite material to be obtained.

The numerical results concern primarily the influence of the model parameters on the stiffness and the hygroexpansion of the homogenised material. The predicted properties are compared with the results of a recently developed analytical model [18] and with certain test results. In addition to the homogenised material properties, the model provides considerably information on the magnitude and distribution of the stresses and strains within the material structure. This can provide estimates of the risk for development of micro-cracks, damage, creep or permanent plastic deformation within the material structure when exposed to various loads or moisture actions.

2 Description of the Model

The model concerns stiffness and hygroexpansion properties. Stiffness is analysed by exposing a square unit cell containing a number of wood fibres and a filling of matrix material to a given deformation in one direction and to zero load in all other directions. The stiffness tensor of the unit composite cell can be obtained by calculating the mean values of the stress and strain vectors for the volume of the cell. The hygroexpansion parameters of the composite cell are obtained by simulating an increase in moisture content and calculating the average strain of the unit cell in each direction.

The numerical modelling involves four steps: modelling the fibre geometry, finite element modelling, solution of the system of equations and postprocessing the results. The fibre and network geometry is created by a preprocessor written in Matlab-code [14]. It defines the volumes of the fibres and of the matrix material and generates input data to the commercial preprocessor Patran, in which the finite element mesh is created, material properties are assigned and the load cases are defined. The finite element analysis is performed by an Abaqus solver, the postprocessing being done using Patran.

2.1 General assumptions

The cross section of the fibres is assumed to be rectangular in shape, corresponding approximately to the shape of the collapsed wood fibres that the paper is made of. The height and the width of the fibres are assumed to be constant and to be the same for all the fibres, which are considered to be long and slender, no fibre ending in the cell. The space within the unit cell not occupied by fibres is occupied completely by matrix material. Thus voids are not considered in the

analysis. The fibre and matrix phases are assumed to be perfectly attached.

The constitutive relations for the fibres and matrix materials are linear elastic orthotropic or transversely isotropic and linear elastic isotropic, respectively, without any rate effect. The hygroexpansion properties of the two constituents are assumed to be linear orthotropic or transversely isotropic and to be isotropic, respectively, as well. Since the composite is formed under high pressure and temperature, an inner prestress within the material structure before any external action is applied appears likely. As long as the performance of the constituents is linear elastic, however, any eigenstress on the homogenised stiffness and expansion properties is without effect.

2.2 Geometry Preprocessing and FE-modelling

The fibre geometry preprocessor enables the user to place the fibres arbitrarily in the unit cell by mouse-clicking on a diagram such as that shown in Figure 1.

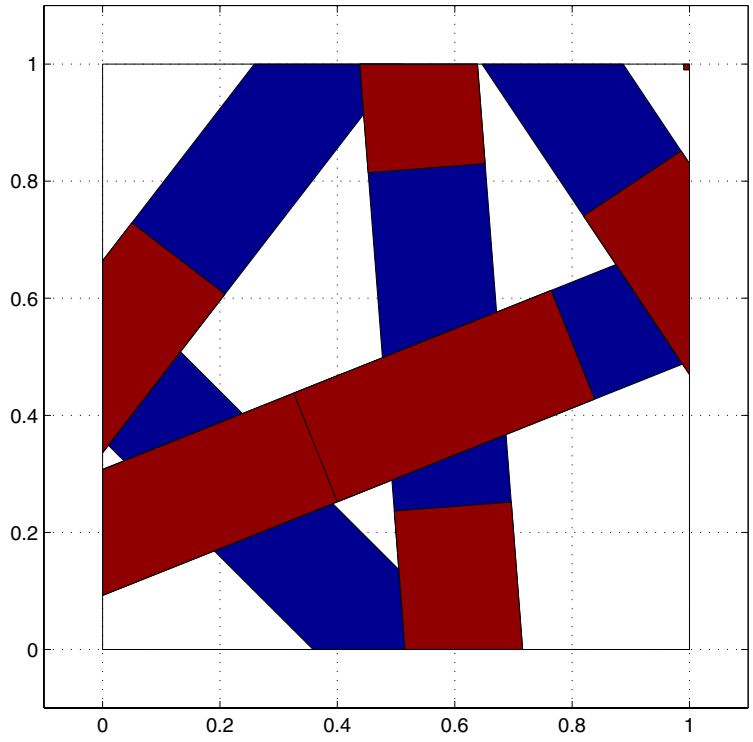

Figure 1: *Fibre geometry preprocessor.*

The first fibre crosses the square in the lowest part of the unit cell, i.e. on the

lowest "floor" of the piece of composite material. The unit cell is $1 \times 1 \times 0.1$ in size, the heigh being given from the fibre thickness, which in this case is 0.05, and the number of "floors". The next fibre generally crosses the first, climbing over it to occupy some volume on the second floor, above the first fibre, in accordance with a smooth third-degree polynomial spline, as shown in Figure 2.

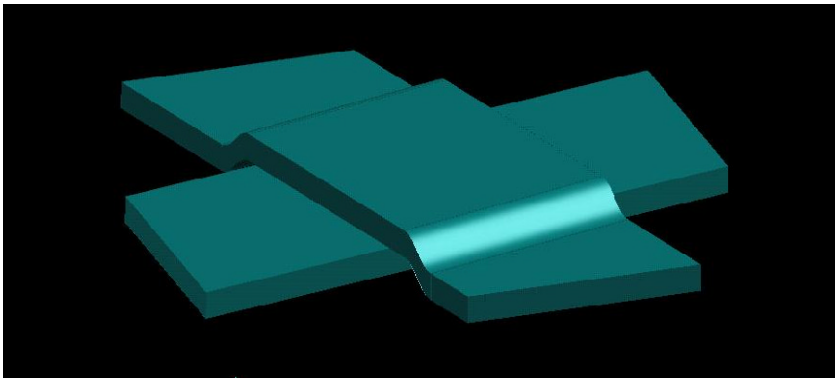

Figure 2: *Fibre crossing.*

As more fibres are added, the geometry typically becomes like that shown in Figure 3. The fibre network preprocessor also creates the geometry of the matrix material, which in boolean terms can be defined as the volume of the unit cell minus the volume of the fibre network, as shown in Figure 4.

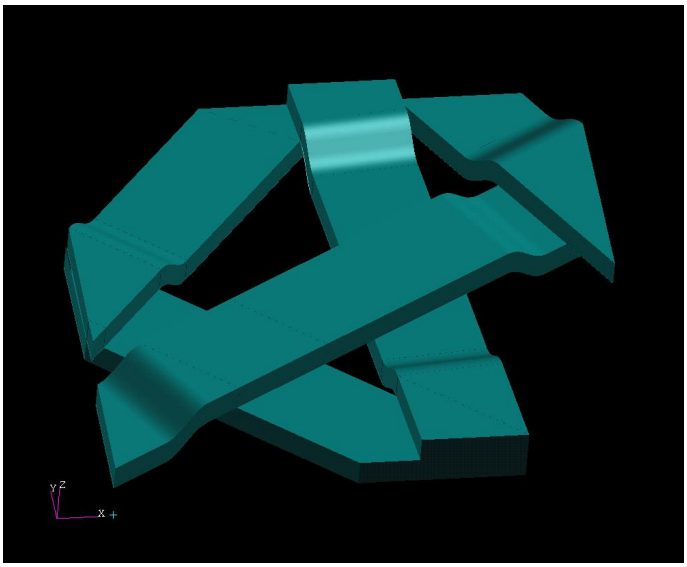

Figure 3: *Network of five fibres.*

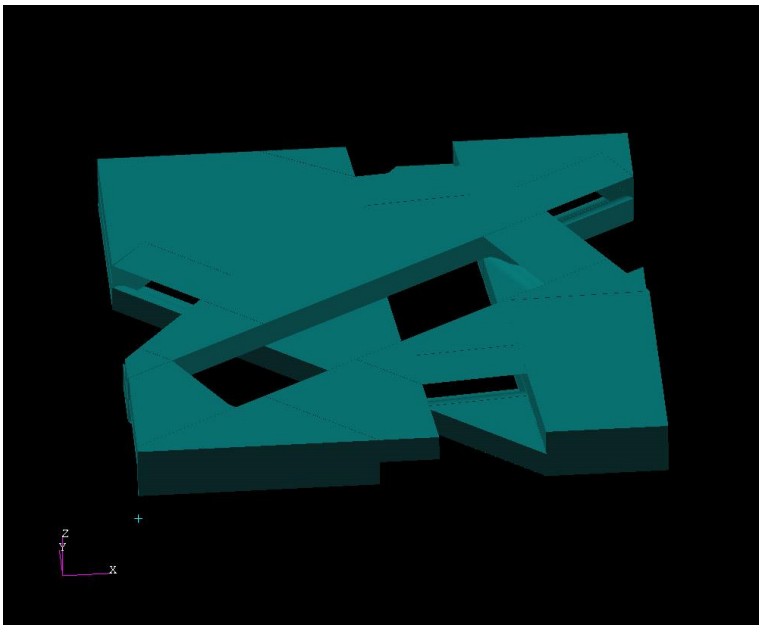

Figure 4: *Geometry of the corresponding matrix material.*

The indata to the preprocessor includes the width, thickness, orientation and location of the fibres, the number of fibres and a slope distance that determines the steepness of the fibre slope that results from the fibres climbing over each other. This determines the maximum of the fibre volume fraction. The maximum of the degree of fibre packing is achieved by use of large fibres placed in a physically realistic way so that they occupy as few "floors" as possible. In Figure 3 five fibres are placed so that they occupy only two "floors". The degree of fibre packing is limited by the slope distances and by the fact that they are assumed to be perpendicular to the longitudinal direction of the fibres. Without using very regular geometries, it is difficult, therefore, to achieve a fibre volume fraction of over 40 %.

2.3 Finite Element Calculations

The finite element mesh is generated in Patran by its producing surface elements that are extruded to the next floor to form hexagonal, iso-parametric 8-node solid elements, see Figure 5. The average element length in the x- and the y-direction is 1/20 the unit cell length. A fibre is modelled by use of about 200 elements. The five-fibre model employs an element thickness of half a "floor". This results in there being four elements in the z-direction, since the model consists of two "floors". The most difficult part of the finite element modelling is

to make the elements between two "floors" compatible, such that the mesh for both "floors" is identical. This is achieved by dividing the "floors" into smaller sections, identical for both "floors". Problems of this sort are based on the fact that Patran is not an ideal solid modeller. The finite element model typically involves about 5000 nodes, which give a system of equations with about 15000 degrees of freedom. These equations are solved in about 20 s, using a single work station.

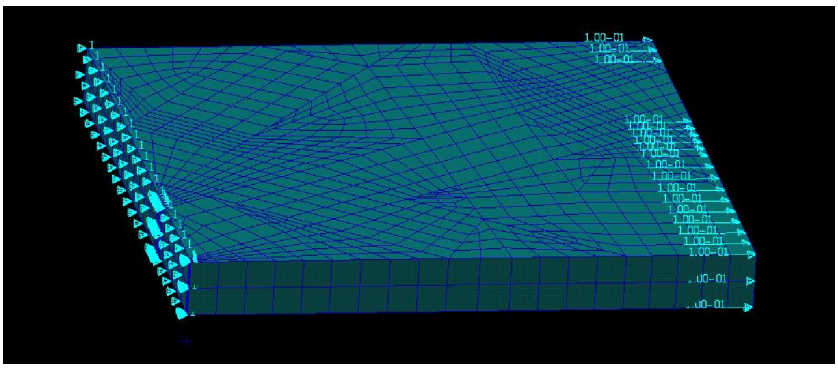

Figure 5: *Unit cell created from the geometries shown in Figure 3 and 4, with a finite element mesh.*

3 Material Properties

The matrix material considered in this study is a phenolic resin assumed to be isotropic, having a Young's modulus of 5.75 Gpa [5] and a Poisson's ratio of 0.3. The hygroexpansion coefficient, β, is defined as the increase in free strain for a given increase in moisture content, expressed in percent. The unit for β is [1/%]. A wood fibre is modelled as a transverse isotropic solid having the material properties shown in Tables 1 and 2. Note that the hygroexpansion coefficients in the transverse directions are estimated to be 26 times as great as those in the longitudinal direction [16]. The adhesion of the constituents is assumed to be perfect and without any chemical interaction or adsorption.

4 Homogenisation Procedure

Homogenisation is performed by exposing the unit cell to a prescribed deformation in the x-, y- and z-directions, respectively. During the prescribed deformation in the x-direction, the two cell boundaries with a normal vector in the

Table 1: *Elastic properties of wood fibres and of phenolic resin.*

Fibre						Matrix	
E_x	$E_y = E_z$	$\nu_{xy} = \nu_{xz}$	ν_{yz}	$G_{xy} = G_{xz}$	G_{yz}	E	ν
[MPa]	[MPa]	[-]	[-]	[MPa]	[MPa]	[MPa]	[-]
40 000	5 000	0.2	0.3	4 000	1 920	5 750	0.3

Table 2: *Hygroexpansion properties of wood fibres, longitudinal and transverse, and of phenolic resin.*

Fibre		Matrix
β_L	β_T	β
[1/%]	[1/%]	[1/%]
0.01	0.26	0.01

x-direction are forced to remain plane. The tangential forces acting on these boundaries are set equal to zero. All the other boundaries are free. The conditions when loading in the y- and z-directions are analogous. A prescribed shear deformation in the x-y-plane is achieved by giving the boundaries with a normal vector in the y-direction a displacement in the tangential, x-direction.

The average strain and the average stress are calculated according to

$$\varepsilon_{ij}^* = \frac{1}{V}\int_V \varepsilon_{ij} dV \qquad (1)$$
$$\sigma_{ij}^* = \frac{1}{V}\int_V \sigma_{ij} dV$$

where ε_{ij}^* are the estimated average strain components and σ_{ij}^* the estimated average stress components calculated over the unit cell volume, V [1]. In the finite element model the integrals are replaced by sums of the stiffnesses and strains of the element, which are constant in the case of 8-node elements. The estimated stiffness components, D_{ijkl}^*, are obtained by use of the corresponding compliance relation

$$\varepsilon_{ij}^* = C_{ijkl}^* \sigma_{kl}^* \qquad (2)$$

for an orthotropic material. From the normal strain and stress components ε_{xx}^*, ε_{yy}^* and ε_{zz}^* and σ_{xx}^* obtained for loading in the x-direction are E_x, ν_{xy} and ν_{xz} easy to calculate. The other stiffness parameters are analogously found from the stress and strain results for loading in the other directions.

The hygroexpansion coefficients are determined by exposing the unit cell to an increase in moisture content and calculating the average strain in all directions. It is assumed here that both constituents have the same increase in moisture content. The constituents increase in the moisture content may in general, depending on the properties of the constituents, be different for a given change in climate.

5 Model Verification and Comparisons

5.1 Simple Two-Fibre Model

The only possibility of reproducing a fibre volume fraction as high as 75 %, which is the volume fraction in the core layer of some HPL materials, is to model only two fibres at a single crossing. Here the width of the fibre is 75 % of the unit cell width and the fibre height is half of the unit cell height. In Table 3 the Young's moduli of this model are compared with the analytical and the measured results. The experimental values are obtained by measuring the core layer of an HPL consisting to 75 % of craft paper and to 25 % of phenolic resin [2]. The analytical model uses the material properties shown in Table 1, along with the same fibre width and height as in the numerical model.

Table 3: *Young's modulus of the composite.*

Numerical		Experimental		Analytical	
E_x [GPa]	E_y [GPa]	E_x [GPa]	E_y [GPa]	E_x [GPa]	E_y [GPa]
15.7	15.2	15.5	10.5	14.4	10.6

The simulated value for E_y here is a bit higher than the values obtained from measurements or from analytical predictions, since the numerical two-fibre model fails to reproduce the fibre orientation distribution correctly. The two-fibre model is equivalent to a cross laminate, whereas the values obtained from the measurements and from the analytical model represent orientation distributions that are continuous and involve 1.8 times more fibres in the x- than in the y-direction.

5.2 Differing Material Structure

The influence of the micro-structure geometry was studied by analysing three different unit cells, each containing five fibres and having an approximate fibre

volume fraction of 45 %. The fibre orientations are plotted in Figure 6.

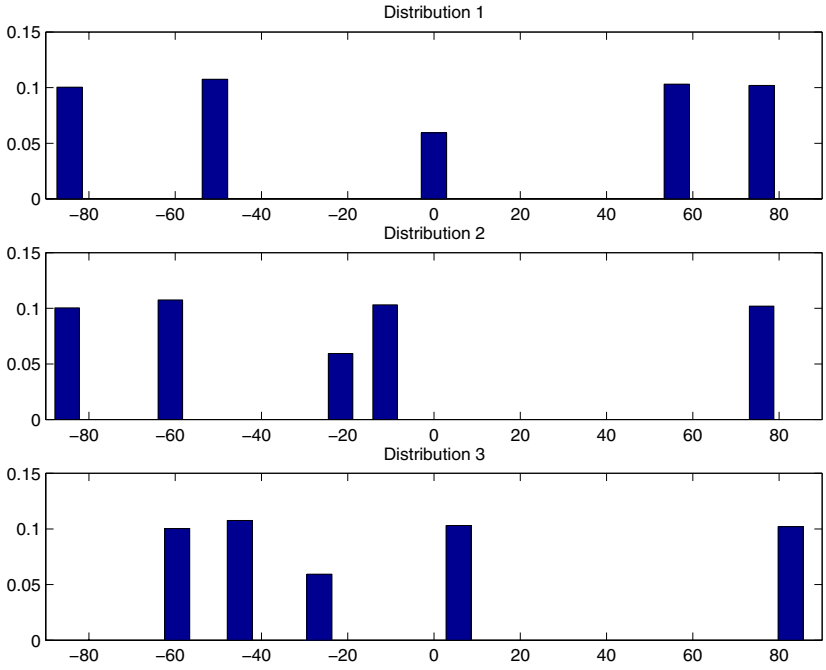

Figure 6: *Fibre angle distribution, $\varphi = 0$ indicating the x-direction. The height of the bar indicates the relative volume of the fibre.*

The Young's moduli, the shear moduli and the hygroexpansion coefficients as calculated for the three fibre distributions are shown in Table 4

Table 4: *Young's moduli and shear moduli in GPa and the hygroexpansion coefficients in 1/% for a composite.*

i	E_x	E_y	E_x	G_{xy}	G_{xz}	G_{yz}	β_x	β_y	β_z
1	9.21	6.70	5.71	1.40	2.25	2.52	0.057	0.051	0.13
2	8.80	11.51	5.71	2.12	2.33	2.42	0.050	0.041	0.12
3	10.41	8.83	5.65	2.56	2.36	2.37	0.053	0.054	-
mean	9.47	9.01	5.69	2.03	2.31	2.44	0.053	0.049	0.13

The variability of the in-plane-stiffnesses, E_x, E_y and G_{xy}, is greater than that of the out-of-plane stiffnesses, E_z, G_{xz} and G_{yz}. This is a reasonable result since it is the in-plane orientation that is varied. Micro-structure variations have less impact on the hygroexpansion coefficients than on the stiffness parameters. In addition, the variability of the hygroexpansion is of the same magnitude in all

three directions. The three structures studied can be regarded as three samples from a single composite material with a globaly uniform fibre orientation distribution. Depending on required accuracy in the calculated homogenised stiffness and hygroexpansion, the results of Table 4 give suggestions about the required number of simulations.

5.3 Differing Matrix Material Stiffnesses

A parameter study on the composite stiffness and the hygroexpansion as a function of the stiffness of the matrix material was carried out using both the analytical model and the numerical model, for a geometry of the type shown in Figure 3 and with a 40 % fibre volume fraction. For the analytical model, fibres of infinite length having an orthotropic fibre distribution were employed. The stiffness of the matrix material was varied from $E_m = 0$ to $E_m = 10$ GPa. The results are shown in Figures 7 and 8.

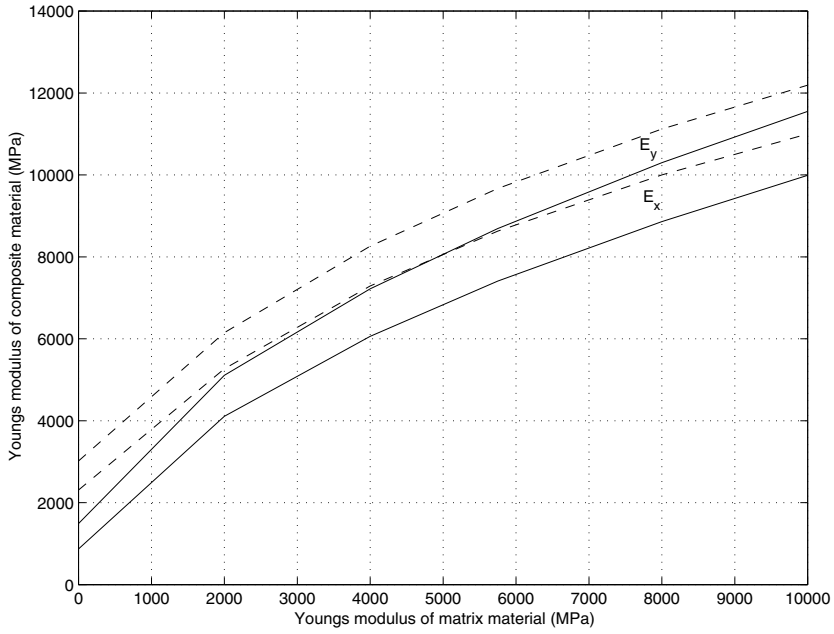

Figure 7: *Young's modulus of the composite in the $x-$ and $y-$ direction. Solid lines = numerical model, dashed lines = analytical model.*

The curves for the Young's moduli in the x- and the y-direction are similar, although the analytical results suggest the stiffness to be greater than that obtained using the numerical model, particularly in the case of low matrix stiffness. This is probably due to the steep slopes found in the numerical model, making

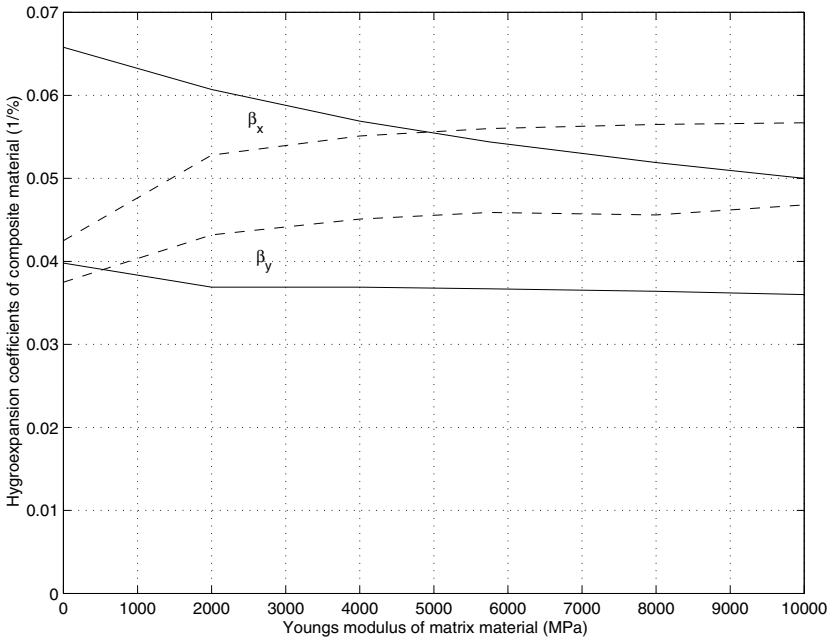

Figure 8: *Composite hygroexpansion coefficients in the $x-$ and $y-$ direction. Solid lines = numerical model, dashed lines = analytical model.*

the fibres bend under longitudinal load. The hygroexpansion coefficient values for the two models are within approximately the same range. There is a basic difference, however, in the prediction of hygroexpansion they give for low matrix material stiffness, E_m. Whereas the analytical model predicts a decrease in hygroexpansion with a decrease in E_m, the numerical model predicts an increase in hygroexpansion with a decrease in E_m. The fact that at low E_m values the hygroexpansion the numerical model predicts is greater than that which the analytical model provides appears logical, since at low E_m values the stiffness which the numerical model predicts is lower.

The stress distribution of the fibre phase of the composite under a prescribed deformation in the x-direction is illustrated in Figure 9. It can be seen that the fibre ranging from the left boundary is exposed to the highest stress, which is logical since the loading is in the x-direction. The material stresses in the matrix are illustrated in Figure 10.

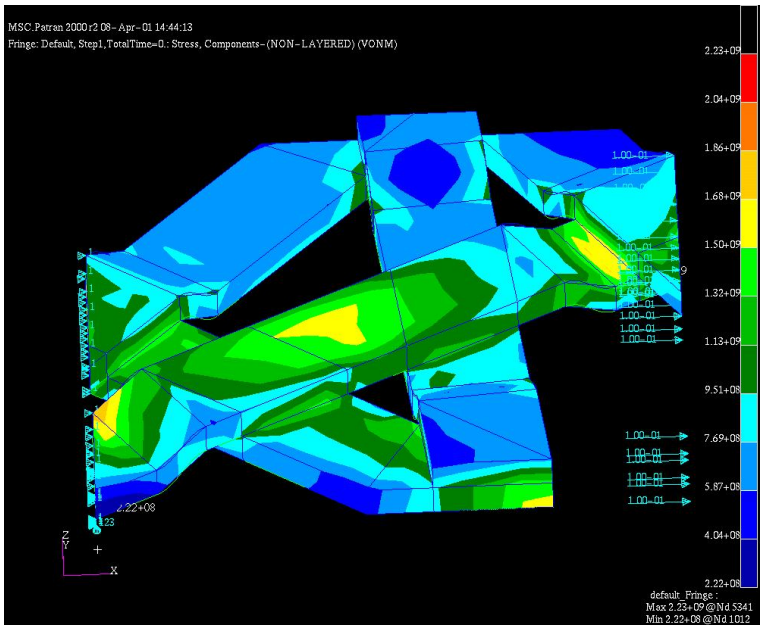

Figure 9: *A von Mises stress distribution of the fibre phase during prescribed elongation in the x-direction. Stress unit: Pa*

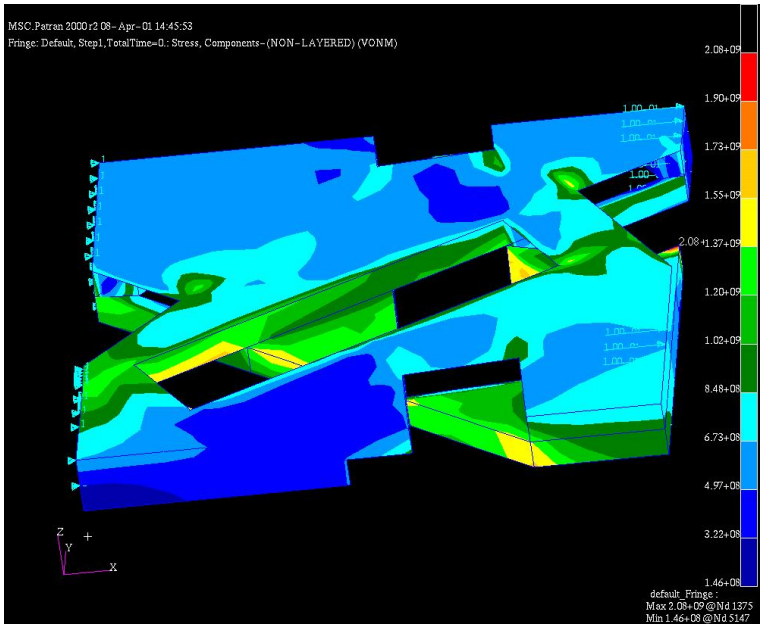

Figure 10: *A von Mises stress distribution of the matrix material phase during prescribed elongation in the x-direction. Stress unit: Pa*

6 Concluding Remarks

A 3D finite element model for the stiffness and hygroexpansion analysis of fibre composite materials was presented. The model provides a good representation of the microstructure of a composite material, such as HLP, and opens up for many possibilities, such as that of creating models of the complex microstructures of various composite materials, perhaps simply on the basis of the information contained in microscopic images. Parameter studies can also be performed of any parameter. The behaviour of new materials which do not yet exists can be analysed as well. The model can also be used to simulate network mechanics models, such as of paper, without the use of matrix material. The model provides reasonably accurate estimates of the stiffness and hygroexpansion of a composite through use of a five-fibre version of the model and of three nominally equal simulations. The five-fibre model may not be sufficient, however, for simulating fibre networks without matrix materials.

In this study only time-independent properties were investigated. The model is also intended, however, for future use in studies of time dependent properties such as creep and mechanosorption which are important for wood and wood composite materials.

7 Future Work

The model studied here was developed as a tool for the analysis of long fibre network composites such as HPL, but it can be developed further so as to achieve an even better representation of the morphology of the composite:

- The fibre packing can be increased to well above the present maximum of about 45% for a multi-fibre random geometry. This can be done by making the fibre shape more flexible, allowing the fibres to be curved in the plane, be twisted or be of varying width and thickness.

- Use of larger unit cells containing more fibres is required to obtain a better representation of a random structure with a continuous fibre orientation distribution. This will result in lesser variability between nominally equal simulations and will accordingly require fewer simulations in order for accurate mean value estimates to be made. The use of larger models will be facilitated by the ongoing development of more efficient finite element software and of faster computers.

- The fibre geometry and its internal structure can be more accurately represented by modelling it as a collapsed pipe in which the inclination of an orthotropic orientation in the fibre walls is induced by the micro-fibril angle.

References

[1] Aboudi, J. (1991). *Mechanics of Composite Materials*, Elsevier, Amsterdam, The Netherlands, 14-18.

[2] Andersson, B. (1999). *Composite Materials' Hygroexpansion Properties.* Master Thesis, Report TVSM-3018, Division of Structural Mechaics, Lund University, Sweden.

[3] Adl Zarrabi, B. (1998). *Hygro-Elastic Deformation of High Pressure Laminates*, Doctoral thesis, Div. of Building Material, Chalmers University of Technology, Göteborg, Sweden

[4] Baldwin, J. D., Altan, M. C., Rajamani, K., (1997). "Structural Analysis of an Injection Molded Short-Fiber-Reinforce Disc". *Journal of Materials Processing and Manufacturing Science*, 6, 123-145.

[5] Barth, Th. (1984). "Der Einfluss der Feuchteaufnahme auf die mechanischen Eigenschaften von Phenolplasten." *Z. Werkstofftech*, Verlag Chemie, Weinheim, Germany, 15, 299-308.

[6] Christman, T., Needleman, A., Suresh, S. (1989). "On Microstructural Evolution and Micromechanical Modelling of Deformation of a Whisker-reinforced Metal-Matrix Composite", *Materials Science and Engineering*, A107, 49-61.

[7] Dasgupta, A., Agarwal, R. K., Bhandarkar, S. M. (1996). "Three-Dimensional Modeling of Woven-Fabric Composites for Effective Thermo-Mechanical and Thermal Properties". *Composites Science and Technology*, 56, 209-223.

[8] Falzon, P. J., Herszberg, I. (1996). "Effects of Compaction on the Stiffness of Plain Weave Fabric RTM Composites". *Journal of Composite Materials*, 30, 1210-1247.

[9] Garnich, M. R., Hansen, C. (1997). "A Multicontinuum Theory for Thermal-Elastic Finite Element Analysis of Composite Materials". *Journal of Composite Materials*, 31, 71-86.

[10] Ghassemieh, E., Nassehi, V. (2001). "Stiffness Analysis of Polymeric Composites Using the Finite Element Model". Advances in Ploymer Technology, 20, 42-57.

[11] Hashin, Z. (1983) "Analysis of Composite Materials, A Survey", *Journal of Applied Mechanics*, 9, 481-505.

[12] Heyden, S. (2000). *Network modelling for the evaluation of mechanical properties of cellulose fibre fluff.*, Doctoral thesis, Report TVSM-1011, Div. of Structural Mechanics, Lund University, Sweden.

[13] Ismar, H., Schroter, F., Streicher, F. (2000). "Modeling and Numerical Simulation of the Mechanical Behaviour of Woven SiC/SiC regarding a Three-Dimensional Unit Cell". *Computational Materials Science*, 19, 320-328.

[14] Matlab - *The language of technical computation.* (1998) The Math Works Inc., Natick, Ma, USA.

[15] Nilsen, N., Niskanen, K. (1996) "A 3D simulation model for paper structure." *Progress in Paper Physics - A Seminar Proceedings.*

[16] Persson, K. (2001). *Micromechanical modelling of wood and fibre properties.* Doctoral thesis, Division of Structural Mechanics, Lund University, Sweden.

[17] Stahl, D. C., Cramer, S. M. (1998). "A Three-Dimensional Network Model for a Low Density Fibrous Composite". *Journal of Engineering Materials and Technology*, 120, 126-130.

[18] Stålne, K., Gustafsson, P. J. (2000). "A 3D Model for Analysis of Stiffness and Hygroexpansion Properties of Fibre Composite Materials", *Journal of Engineering Mechanics*, in press.

[19] Termonia, Y. (1994). "Structure-Property Relationships in Short-Fiber-Reinforced Composites". *Journal of Polymer Science, Part B: Polymer Physics*, 32, 969-979.

[20] Thom, H. (1999). "Finite Element Modeling of Plain Weave Composites" *Journal of Composite Materials*, 33, 1491-1510.

[21] Toll, S. (1998). "Packing Mechanics of Fiber Reinforcements". *Polymer Engineering and Science*, 38, 1337-1350.

[22] Tucker, C.L., Liang, E. (1999). "Stiffness Predictions for Unidirectional Short-Fiber Composites: Review and Evaluation" *Composites Science and Technology* 59, 655-671.

[23] Whitcomb, J. D., Chapman, C. D., Tang, X. (2000). "Derivation of Boundary Conditions for Micromechanics Analyses of Plain and Satin Weave Composites". *Journal of Composite Materials*, 34, 724-747.

[24] Zeman, J., Sejnoha, M., (2001). "Numerical Evaluation of Effective Elastic Properties of Graphite Fiber Tow Impregnated by Polymer Matrix". *Journal of the Mechanics and Physics of Solids*, 49, 69-90.